

UC Davis

UC Davis Previously Published Works

Title

Requirements for Neurogenin2 during mouse postnatal retinal neurogenesis

Permalink

<https://escholarship.org/uc/item/42h464sk>

Journal

Developmental Biology, 442(2)

ISSN

0012-1606

Authors

Kowalchuk, Angelica M
Maurer, Kate A
Shoja-Taheri, Farnaz
[et al.](#)

Publication Date

2018-10-01

DOI

10.1016/j.ydbio.2018.07.020

Peer reviewed



HHS Public Access

Author manuscript

Dev Biol. Author manuscript; available in PMC 2019 October 15.

Published in final edited form as:

Dev Biol. 2018 October 15; 442(2): 220–235. doi:10.1016/j.ydbio.2018.07.020.

Requirements for *Neurogenin2* during mouse postnatal retinal neurogenesis

Angelica M. Kowalchuk¹, Kate A. Maurer^{2,1}, Farnaz Shoja-Taheri^{1,2}, and Nadean L. Brown^{1,2,*}

¹Department of Cell Biology and Human Anatomy, University of California-Davis, Davis, CA, 95616

²Division of Developmental Biology, Cincinnati Children's Hospital Research Foundation; Cincinnati, OH 45229

Abstract

During embryonic retinal development, the bHLH factor *Neurog2* regulates the temporal progression of neurogenesis, but no role has been assigned for this gene in the postnatal retina. Using *Neurog2* conditional mutants, we found that *Neurog2* is necessary for the development of an early, embryonic cohort of rod photoreceptors, but also required by both a subset of cone bipolar subtypes, and rod bipolars. Using transcriptomics, we identified a subset of downregulated genes in P2 *Neurog2* mutants, which act during rod differentiation, outer segment morphogenesis or visual processing. We also uncovered defects in neuronal cell culling, which suggests that the rod and bipolar cell phenotypes may arise via more complex mechanisms rather than a simple cell fate shift. However, given an overall phenotypic resemblance between *Neurog2* and *Blimp1* mutants, we explored the relationship between these two factors. We found that *Blimp1* is downregulated between E12-birth in *Neurog2* mutants, which probably reflects a dependence on *Neurog2* in embryonic progenitor cells. Overall, we conclude that the *Neurog2* gene is expressed and active prior to birth, but also exerts an influence on postnatal retinal neuron differentiation.

Keywords

Neurog2, *Blimp1*, *Prdm1*; rod photoreceptor; bipolar cell; retina

Introduction

The vertebrate eye contains a precise retinal circuitry for the detection and processing of visual stimuli. Failure to produce and maintain the correct proportions of each retinal cell type contributes to vision impairment and blindness. These retinal cell types (six neuronal

*Corresponding author. Phone: 530-752-7806. nlbrown@ucdavis.edu.

¹Present address: Medpace Central Laboratories Cincinnati, OH

²Present address: Department of Biomedical Engineering Emory University, Atlanta, GA

Publisher's Disclaimer: This is a PDF file of an unedited manuscript that has been accepted for publication. As a service to our customers we are providing this early version of the manuscript. The manuscript will undergo copyediting, typesetting, and review of the resulting proof before it is published in its final citable form. Please note that during the production process errors may be discovered which could affect the content, and all legal disclaimers that apply to the journal pertain.

and one glial) are derived from a common pool of multipotent progenitor cells that arise in an overlapping temporal sequence (Sidman, 1961; Young, 1985). Mouse retinal development occurs over a nearly six week period of time, during which retinal ganglion cells (RGCs), horizontal cells, cone photoreceptors, some amacrine and a subset of rod photoreceptors differentiate before birth, while the remainder of amacrine, the majority of rods, bipolar cells and Muller glia differentiate postnatally (Sidman, 1961; Young, 1985). In mice, retinal neurogenesis begins at the center of the optic cup at embryonic day 11 (E11) and expands peripherally, reaching the distal-most region by E16 (Hinds, 1968; Sidman, 1961). Retinal progenitor cells (RPCs) are generally instructed by intrinsic factors about their cell fate, and by extrinsic signals regarding temporal competence states and the overall proportion of each cell class (Cepko, 2014; Cepko et al., 1996).

Basic helix-loop-helix (bHLH) transcription factors are well established intrinsic regulators of neurogenesis. Two bHLH factors, *Atoh7* and *Neurogenin2* (*Neurog2*), are expressed by RPCs that produce the first RGCs (Brown et al., 1998; Brown et al., 2001b; Gradwohl et al., 1996; Sommer et al., 1996; Wang et al., 2001; Yan et al., 2001). Previously *Neurog2* was shown to activate *Atoh7* transcription directly, plus control the spatiotemporal progression of the initial wave of retinal neurogenesis (Hufnagel et al., 2010; Skowronska-Krawczyk et al., 2009). However, *Neurog2* does not instruct early cell fates per se, given that in E18.5 *Neurog2* germline mutants there was only a 2% increase in RGCs, and no impact on the proportions of RPCs, cone photoreceptor, amacrine or horizontal neurons (Hufnagel et al., 2010). However, the requirements for this gene in the postnatal retina have not been explored, since germline mutants die at birth (Fode et al., 1998).

Here we assessed the role of *Neurog2* during the later phases of retinal development, using a conditional allele and two retinal Cre drivers (Hand et al., 2005; Prasov and Glaser, 2012; Rowan and Cepko, 2004). We found that only the earliest differentiating rod photoreceptors require *Neurog2*, consistent with the *Neurog2* retinal lineage producing mostly rods at E17.5 (Brzezinski et al., 2011), and the complete downregulation of this gene soon after birth. Although the proportion of rods that depend on *Neurog2* is relatively small, our postnatal day 2 (P2) transcriptomic analysis of *Neurog2* conditional mutants revealed that the main class of down-regulated transcripts are rod-specific. Somewhat paradoxically, we also found additional retinal phenotypes that arose after *Neurog2* expression is normally abolished. These included a significant loss of several cone bipolar subtypes, an increase in rod bipolar neurons, and defects in neuronal culling. Our data also show that the photoreceptor-bipolar fate determinant, *Prdm1/Blimp1* (Brzezinski et al., 2010; Brzezinski et al., 2013; Katoh et al., 2010; Mills et al., 2017; Wang et al., 2014) is downregulated embryonically in *Neurog2* mutants, well ahead of the rod and bipolar phenotypes. Although the cell classes affected are similar between *Neurog2* and *Blimp1* retinal mutants, the *Neurog2* phenotypes were considerably milder and seem to primarily impact differentiation. Overall, we conclude that *Neurog2* is required during postnatal retinal differentiation, but that other molecular pathway(s) likely act redundantly with *Neurog2*. Our findings provide an entry point for better elucidation of the gene networks that comprehensively regulate rod, cone and rod bipolar development.

Materials and Methods

Mice and BrdU injections

Mouse lines used in this study were a *Neurog2^{GFP}* germline allele (*Neurog2^{tm4Fgu}*), maintained on an ICR background (Seibt et al., 2003), *Neurog2^{CKO}* allele (*Neurog2^{tm5(Neurog2^{Fgu})}*) maintained on a CD-1 background (Hand et al., 2005), *Chx10-Cre* transgenic line (*Tg(Chx10-EGFP/cre;-ALPP)2Clc*) maintained on a CD-1 background (Rowan and Cepko, 2004), and a BAC-Tg *CrxCre* mouse (*Tg(Crx-cre)352Gla*) maintained on a C57BL/6 background (Prasov and Glaser, 2012). PCR genotyping was performed as described (Hand et al., 2005; Prasov and Glaser, 2012; Rowan and Cepko, 2004; Seibt et al., 2003). Timed matings were used to determine embryonic age, with E0.5 as the date of the vaginal plug was noted. In retinal birthdating experiments, a 10mg/ml BrdU solution (0.1mg/g body weight in 0.9M NaCl) was injected in pregnant dams carrying E17.5 litters and P21 eyes collected for analysis. Postnatal P3 pups were injected intraperitoneally with 40µl of the same BrdU solution and eyes collected at P21. All mice were housed and cared for in accordance with the guidelines provided by the National Institutes of Health, Bethesda, Maryland, and the Association for Research in Vision and Ophthalmology, and conducted with approval and oversight from the UC Davis Institutional Animal Care and Use Committee.

Immunohistochemistry

Embryonic and postnatal tissues were fixed in 4% paraformaldehyde for 30 minutes at 4°C and processed, embedded, sectioned and antibody labeled as in Mastick and Andrews (2001). Anti-BrdU labeling conditions were as in Le et al. (2006). Primary antibodies used were rabbit anti-Arrestin 3/Cone Arrestin (1:7000, Millipore Cat#:AB15282), rat anti-Blimp1/Prdml (1:100, Santa Cruz Cat#:sc-47732), rat anti-BrdU (1:100, AbD Serotec Cat#:OBT0030), sheep anti-Chx10/Vsx2 (1:700, Abeam Cat#:AB16141), rabbit anti-cleaved PARP (1:500, Cell Signaling Cat#:9544), rabbit anti-Cre (1:500, Covance Cat#:MMS-106R), rabbit anti-Crx (1:1000, a gift from Cheryl Craft, USC; Fig 1 and Suppl Fig. 3), rabbit anti-Crx (1:500, Santa Cruz Cat#:sc-30150 (discontinued); Suppl Fig. 2), chick anti-GFP (1:3000, Aves Cat#:GFP-1020), mouse anti-Neurog2 (1:1000, R&D Systems Cat#:MAB3314), mouse anti-Nr2e3 (1:200, R&D Systems Cat#:PP-H7223-00), goat anti-Otx2 (1:200, R&D Systems Cat#:BAF1979), mouse anti-Pax6 (1:200, Santa Cruz Cat#:sc-32766), rabbit anti-Pax6 (1:1000, Covance Cat#:PRB-278P), mouse anti-protein kinase C α (1:200, Sigma-Aldrich Cat#:P5704), rabbit anti-Sox9 (1:200, Millipore Cat#:AB5535), and rabbit anti-Vsx1 (1:200, Clark et al., 2008). Sections were then incubated with directly conjugated Alexafluor secondary antibodies (1:400, Jackson ImmunoResearch or Molecular Probes) or biotinylated secondary antibodies (1:500, Jackson ImmunoResearch or ThermoScientific) followed by Alexafluor conjugated streptavidin (1:500, Jackson ImmunoResearch). In Figure 5D-F, rabbit anti-cPARP was directly conjugated with a Zenon Rabbit IgG Alexa Fluor 594 Labeling Kit (Molecular Probes Cat: Z-25307). Nuclei were labeled with DAPI (1:1000 dilution of a 1mg/ml solution, Sigma-Aldrich Cat#:28718-90-3).

Microscopy and Cell Counting

Microscopy was performed with either a Zeiss fluorescent microscope, Zeiss camera and Apotome deconvolution device or a Leica DM5500 microscope, equipped with a SPEII solid state confocal and processed using Leica LASAF and Adobe Photoshop (CS4) software programs. All digital micrographs were equivalently adjusted among genotypes for brightness, contrast and pseudo-coloring.

For quantification of marker labeled cells, 3 individuals per genotype were analyzed using at least 2 sections per individual. Equivalent anatomical depth in the retina was determined by proximity to the optic nerve. Cell counts were performed using the count tool in Adobe Photoshop CS4. Statistical significance was determined using IBM SPSS Statistics (v. 24) with either an unpaired 2 sample T-Test with a Welsh correction or one-way ANOVA with Welsh's correction and a Tukey post hoc test.

Western Blots

P2 retinal pairs were sonicated in RIPA buffer with protease inhibitors (Complete, Sigma Cat# 11697498001) and processed as described (Prasov et al, 2010). Total retinal protein (25µg/lane) was loaded on a NuPage 4–12% Bis-Tris gel (Invitrogen Cat#:NP0322BOX), electrophoresed and transferred to a nitrocellulose membrane (Invitrogen Cat#:LC2000). Blots were blocked in 4% milk/0.1M Tris (pH 7.4)/0.15MNaCl/0.1% Tween20, probed with rat anti-Blimp1/Prdml (1:100, Santa Cruz Cat#:sc-47732) and mouse anti-β-actin (1:4000, Sigma-Aldrich Cat#:A1978), and visualized with IRDye 800CW (1:15,000, Li-Cor Cat#:926–32219) and IRDye 680RD (1:20,000, Li-Cor Cat#:926–68022), respectively, on the Li-Cor Odyssey Clx Imaging System. Densitometric analysis was performed using the Image Studio Lite software (v. 5.2).

RNA-sequencing and Quantitative PCR

RNA-sequencing was performed on *Neurog2^{CKO/CKC}*, *Chx10-Cre;Neurog2^{CKO/CKO}* and retinas (n = 5 biologic replicates/genotype). Total RNA was extracted from individual pairs of retinal tissue using the Zymo Research Quick RNA miniprep kit (Cat#:R1055). RNA concentrations were determined with a Qubit 3.0 Fluorometer and Molecular Probes Qubit RNA HS Assay kit (Cat#:Q32852). Fifteen samples with RIN values > 7.9 were sent to the CCHMC DNA sequencing Core for library preparation and paired end, poly-A stranded RNA sequencing on an Illumina HiSeq 2500, at a 30 million read depth. Reads were aligned with BWA and Bowtie programs to the mm10 genome. Aligned reads were then analyzed for differentially expressed transcripts using the CuffDiff program in the Galaxy online bioinformatics package (www.usegalaxy.org). Differentially expressed transcripts were initially evaluated with an adjusted p-value cutoff of q < 0.05. Analysis was broadened to a significance of p < 0.05 for some transcripts with the requirement of validation. Transcripts were grouped by ontology using PANTHER (www.geneontology.org) and ranked for fold enrichment, which is the proportion of genes in a particular functional group, compared to the number of genes in that group expected in a random list of genes. For genes showing significant changes, sequence reads were aligned to mm10 were visualized with the Integrative Genomics Viewer (IGV) browser (v. 2.3)(Robinson et al., 2011; Thorvaldsdottir et al., 2013). RNA seq data in this publication have been deposited in NCBI's Gene

Expression Omnibus (Edgar et al., 2002) and accessible by GEO Series accession number GSE103457 (<https://www.ncbi.nlm.nih.gov/geo/query/acc.cgi?acc=GSE103457>).

Validation of RNA-sequencing results was performed by quantitative PCR by reverse transcribing P2 total retinal RNA into cDNA using the Bio-Rad iScript cDNA Synthesis Kit (Cat#: 170–8891) and performing qPCR with primer sets listed in Supplemental Table 1 and Applied BioSystems Fast Sybr Green Master Mix (Cat#:4385614) on an Applied BioSystems StepOnePlus machine. Relative Quantification (RQ) values were calculated using a comparative CT method (Livak and Schmittgen,2001) with β -actin as an endogenous control. Statistical significance was determined using IBM SPSS Statistics (v. 24) with an unpaired 2 sample T-Test and Welsh correction.

Results

***Neurog2* is required during prenatal rod photoreceptor genesis**

Multiple studies have documented *Neurog2* expression in retinal progenitor cells (RPCs) between E11 to P2 (Akagi et al., 2004; Brown et al., 1998; Brzezinski et al., 2011; de Melo et al., 2018; Ma et al., 1996; Skowronska-Krawczyk et al., 2009), although there is conflicting data about when this gene shuts off between postnatal day 0 (P0) and P2. So, we labeled early postnatal retinal cryosections with a validated antibody and directly compared *Neurog2* expression. At P0, we readily saw a cohort of *Neurog2*⁺ RPCs, but at P2 the retina was completely devoid of expression (Suppl Fig 1). From this, we conclude that *Neurog2* becomes downregulated at P1. In addition, there are some key characteristics of the *Neurog2* retinal lineage relevant for interpreting conditional mutant phenotypes. First, all adult retinal neuron arises from RPCs that previously expressed *Neurog2*, but the proportions of cell types produced varies with embryonic age (Brzezinski et al., 2011; Ma and Wang, 2006). For example, E12/E13 *Neurog2*-expressing RPCs mostly give rise to RGCs, but by E17.5, this lineage mainly produces rods. Second, adult retinal *Neurog2* lineage-marked cells are in 1–3 cell clones, suggesting they exited the cell cycle and differentiated soon after labeling (Brzezinski et al., 2011). Together, these data reveal a narrow developmental window when *Neurog2* might influence rod development (E14-P0). Although this interval overlaps the period of rod birthdates (E13-P7), only a small number of rods differentiate prenatally (Carter-Dawson and LaVail, 1979; Cepko et al., 1996; Morrow et al., 1999; Young, 1985). For these reasons, it was plausible that *Neurog2* mutants might exhibit a relatively small rod phenotype.

Previously we quantified *Rxrg*⁺ cone photoreceptors in E18.5 *Neurog2* germline mutants (Hufnagel et al., 2010 and regraphed in Fig. 1E), but rod photoreceptor markers were not evaluated. To integrate our conditional mutant analyses with this previous study, we first quantified the percentages of *Crx*⁺ (photoreceptor precursors) and *Nr2e3*⁺ (rods) cells in E18.5 *Neurog2*^{GFP/+} and *Neurog2*^{GFP/GFP} eyes (Fig. 1A-E). We found a small, but significant, decrease in rods in *Neurog2*^{GFP/GFP} mutants (4.0%, compared to 5.7% in controls, Fig 1E), and fewer *Crx*⁺ cells, although this was not statistically significant (mutants = 22.9% versus controls = 24.4%).

Retinal-specific removal of *Neurog2* revealed defects in rod and bipolar neurogenesis

Then to fully evaluate postnatal retinogenesis, we used *Neurog2*^{CKO/CKO} mice, and two different retinal Cre lines. Most experiments utilized BAC-Tg Chx10-Cre, which deletes genes in the majority of E9-P2 RPCs (Suppl Fig 2A,2B), as well as in nascent bipolar neurons (Suppl Fig 2C,2D) (Rowan and Cepko, 2004). At E14.5, this Cre driver induced the complete cell autonomous loss of *Neurog2* expression (Suppl Fig 2E–2F', 2I). We also evaluated a second cre driver, BAC-Tg Crx-Cre, because it more specifically removes gene activity from the precursors of cones, rods and bipolar cells (Prasov and Glaser, 2012), and does not become active until after the initial wave of neurogenesis, which depends on *Neurog2* (Hufnagel et al., 2010). Here too, we saw a cell autonomous loss of *Neurog2* expression (Suppl Fig 2G–2I) but noted that only a subset of embryonic RPCs coexpress Crx and *Neurog2* proteins (Suppl Fig 2 and Suppl Fig 3; see Methods about different Crx antibodies used). This suggested that Crx-Cre can only delete *Neurog2* within a relatively small fraction of cells that commit to photoreceptor or bipolar fates. Intriguingly, we also observed that both Cre lines appear to also produce a non cell-autonomous loss of *Neurog2* expression (Suppl Fig 2I). We concluded that Chx10-Cre is the more robust tool, and so limited our Crx-Cre;*Neurog2* mutant analyses to confirming the adult phenotypes identified with Chx10-cre.

We first compared histologic sections from Chx10-Cre; *Neurog2*^{CKO/+} or Chx10-Cre;*Neurog2*^{CKO/CKO} P21 retinas (Fig. 2A,B), but no obvious defects were apparent (Figs. 2A,B). Next, we used cell type specific antibody markers to label and quantify rod photoreceptors (Fig. 2C,D), bipolar cells (Fig. 2E,F), Muller glia (Fig. 2G,H), and amacrine cells (Fig. 2I,J) at P21. Mature rod photoreceptor nuclei have a stereotypical laminar position in the outer nuclear layer (ONL), and a specific morphology of central condensed heterochromatin and surrounding euchromatin (Carter-Dawson and LaVail, 1979; Helmlinger et al., 2006). Yet these neurons are a challenge to quantify, even when specifically labeled, due to very dense packing in the ONL. So, we opted to exclude cone photoreceptors by labeling sections with anti-Arr3 (Keeley et al., 2013; Liu et al., 2012; Wu et al., 2013), quantifying the number of cones and then subtracting from the total number of DAPI-labeled ONL nuclei in 400X image fields (Fig 2C,D,K), to arrive at the percentage of rods. The INL cell types were quantified directly (percentage of marker+/total INL DAPI+ among genotypes), by labeling with specific markers.

We observed a statistically significant reduction of rod photoreceptors in *Neurog2* mutants (Control = 98.0%; Chx10-Cre ;*Neurog2*^{CKO/CKO} = 97.1%) (Fig. 2K). We also noted a significant increase in Vsx2+ bipolar cells (Controls = 43.2%; Chx10-Cre;*Neurog2*^{CKO/CKO} = 53.4%) (Fig. 2L). The Muller glia and amacrine cells were unaffected by *Neurog2* ablation (Fig. 2N,O). These outcomes were confirmed in P21 Crx-Cre; *Neurog2*^{CKO/CKO} eyes (Fig 2, n=3/genotype). Overall, for either conditional mutant, there was a 0.9% loss in rod photoreceptors and a 10.2% increase in bipolar cells. On average, rod photoreceptors comprise 97.2% of all photoreceptors and >70% of all retinal cells (Carter-Dawson and LaVail, 1979; Jeon et al., 1998; Young, 1985). Bipolar cells constitute 41% of the inner nuclear layer but only 8% of all retinal cells (Jeon et al., 1998; Kim et al., 2008; Young, 1985). Despite obvious proportionality differences for these cell classes in the mature retina,

we noted that the average number of rod photoreceptor cells lost from Chx10-Cre; *Neurog2*^{CKO/CKO} eyes roughly balanced the average number of ectopic Vsx2+ bipolar neurons (Fig. 2M; n = 3 control animals, n = 4 mutants).

Rod and bipolar neuronal birthdating in *Neurog2* retinal mutants

The adult retinal cell type analyses implied that the loss of rods and increase in bipolar neurons might be coordinated events. To address this possibility, we performed *in vivo* BrdU birthdating (Miller and Nowakowski, 1988; Nowakowski et al., 1989) at two ages: E18.5 when the rod defect was first noted (Fig. 1), and P3, the peak of bipolar neurogenesis (Young, 1985). However, to ensure sufficient time for BrdU incorporation in fetuses close to birth, we injected pregnant mice at E17.5. All injected mice were reared to P21 and their eyes collected for evaluation. Once again, we estimated the number of rods by subtracting Arr3+ cone cell counts from the total number of DAPI-labeled ONL nuclei. When we examined labeled retinal sections for BrdU incorporation, we found zero Arr3+ cones birthdated at E17.5 or P3 (n = 3 per age/genotype). Next, the percentage of birthdated rods was determined by counting BrdU+ DAPI-labeled (*Arr3-negative*) ONL nuclei (Fig. 3A-C, arrows in Fig 3A) and dividing this number by the total number of ONL nuclei. E17.5 birthdated rods decreased from 3.4% (wild type) to 1.8% (*Neurog2* mutant), although this shift was not statistically significant (Fig. 3G). For P3 bipolar neuron birthdates, we quantified Vsx2+ BrdU+ nuclei and divided by the total number of INL DAPI+ nuclei (Fig. 3D-F). Here we found a significant increase in birthdated bipolars, from 5.9% in controls to 10.0% in mutants (Fig. 3H). To understand if there was a temporal delay in rod photoreceptor birthdates, we also quantified them at P3 (Suppl Fig 4D-F,H); and also tested for precocious bipolar neurogenesis at E17.5 (Suppl Fig 4-C,G). However, there was no support for either situation, further highlighting that each cell type only requires *Neurog2* at a particular age.

Bipolar neuron subtypes have different requirements for *Neurog2*

To explore the bipolar phenotype further, we independently confirmed an overall increase in bipolar neurons in *Neurog2* mutant retinas by labeling with an Otx2 antibody (Fig. 4A,B). Otx2 normally is expressed by photoreceptors and bipolar cells (Fossat et al., 2007; Nishida et al., 2003), which are distinguished by their ONL versus INL locations. We noted a significant increase (from 41.7% in controls to 51.8% in *Neurog2* mutants) in INL Otx2+ cells (Fig. 4E). In order to gain more insight into bipolar subtypes, we also labeled adult retinas with antibodies against Otx2 and PKC (Fig. 4A,B), whose coexpression demarcates rod bipolar cells; and also, with anti-Vsx1 (Fig. 4C,D) which is expressed by three cone bipolar subtypes. We found a significant increase in the percentage of Otx2+PKC+ cells (11.9% in controls to 18.6% in *Neurog2* mutants; Fig. 4F). However, Vsx1+ cells were markedly decreased (16.6% in controls to 11.6% in *Neurog2* mutants; Fig. 4G). In addition, there was a significant loss of *Vsx1* mRNA in P10 *Neurog2* conditionally mutant retinas (Fig. 4H). We conclude that the loss of *Neurog2* causes complex changes among bipolar subtypes, rather than simply inducing a generic overproduction.

Neurog2 is required for postnatal retinal cell viability

Multiple retinal neuron cell classes are initially overproduced and their final numbers are corrected postnatally, for example, excess bipolar neurons are culled at P9-P10 (Young, 1984). Because of this, there are more bipolar neurons in the P7 retina, than there are after P10. To address the possibility that the percentage of P21 bipolars underrepresented the magnitude of ectopic bipolar neurons that arise in *Neurog2* conditional mutants, we next compared the proportions of P7 bipolar neurons among genotypes. However, at this age, *Vsx2* expression in nascent bipolars and a cohort of late RPCs are not easily distinguished (Burmeister et al., 1996; Liu et al., 1994). So, we colabeled P7 retinal sections with *Vsx2* and *Otx2*, with the latter expressed by both photoreceptors and bipolars (Muranishi et al., 2011; Nishida et al., 2003). Thus, only bipolar neurons express both *Otx2* and *Vsx2* (Fig. 5A-C). We noted a significant increase in bipolar cells in *Chx10-Cre;Neurog2^{CKO/CKO}* (48.6%) over controls (40.6%) (Fig. 5J), which approximated our P21 data (Fig. 2).

To test the possibility that *Neurog2* (directly or indirectly) regulates some aspect of bipolar neuron culling, we assayed apoptosis in *Neurog2* conditional mutants, by colabeling P9 retinal sections with the apoptosis marker anti-cleaved PARP and the bipolar marker *Vsx2* (Fig. 5D-F). We found a significant reduction in bipolar cell death in mutants, relative to controls (Fig. 5K). Then we compared rod cell death at this same age (Fig. 5G-I). This experiment required colabeling retinal sections with two rabbit primary antibodies. To eliminate secondary antibody cross-reactivity, we directly conjugated the cPARP antibody to Alexa Fluor 594. Upon marker quantification, we also noted a statistically significant increase in dying rod photoreceptors (cPARP+Arr3-) in mutant retinas (Fig. 5K).

Blimp1 is downregulated in Neurog2 mutant retinas

The zinc finger transcriptional repressor *Blimp1* (*Prdm1*) normally acts in a subset of retinal precursors that differentiate as photoreceptors (Brzezinski et al., 2010; Katoh et al., 2010; Wang et al., 2014). When *Blimp1* expression is lost, retinal cells erroneously develop as bipolar neurons, with these shifts occurring at a 1:1 ratio (Brzezinski et al., 2010; Brzezinski et al., 2013; Katoh et al., 2010; Wang et al., 2014). Given an overall similarity between the *Neurog2* and *Blimp1* retinal phenotypes, we wished to explore the relationship between these two transcription factors. To determine the extent to which RPCs coexpress *Blimp1* and *Neurog2*, we colabeled E14.5 *Neurog2^{CKO/CKO}* control retinas with specific antibodies for these proteins. We found that 38% of the *Blimp1*+ population coexpress *Neurog2* (Fig. 6C), while 42% of the *Neurog2*+ population coexpresses *Blimp1* (Fig. 6D). Then, we asked whether *Blimp1* expression depends on *Neurog2* activity, by quantifying the percentage of *Blimp1*+ cells in control versus *Neurog2* mutants, at both E14.5 and P2, which corresponds to the peak of *Neurog2* and *Blimp1* expression, respectively (Fig. 7A-F). There was a significant decrease in the proportion of *Blimp1*+ cells in E14.5 *Neurog2* mutant retinas (8.5%) when compared to wild type controls (10.0%)(Figs. 7A-C). The loss of *Blimp1*+ cells was more prominent at P2, immediately after *Neurog2* expression had ceased (58.0% in control, 42.2% in *Chx10-Cre;Neurog2^{CKO/CKO}* mutants)(Figs. 7D-F).

In a separate study about the initial wave of retinal neurogenesis, we performed a transcriptomics analysis of purified GFP+ RPCs from E12.5 *Neurog2^{GFP/+}* and

Neurog2^{GFP/GFP} eyes (Maurer et al., 2018). Here *Blimp1* mRNA levels were already significantly reduced in the absence of *Neurog2* (n = 3 biologic replicates/genotype). This outcome was validated by qPCR, using total RNA from purified E12.5 GFP+ RPCs (Fig. 7G; n = 3/genotype). We also used qPCR to measure *Blimp1* mRNA levels at P2, but by this age, *Blimp1* mRNA expression had returned to normal in *Neurog2* conditional mutants (Fig. 7G). This suggested differential regulation of *Blimp1* mRNA and protein between early versus late retinal development. So, we quantified the Blimp1+ cells, via antibody labeling of *Neurog2* P2 conditional mutant cryosections (Figs 7D-F) and found a significant reduction in the percentage of Blimp1+ cells, which was further verified by measuring Blimp1 protein levels. Using densitometry on P2 retinal protein western blots (Fig 7H), we noted a 44% loss of Blimp1 protein in *Neurog2* mutants compared to controls (Fig. 7I; n = 3 biologic replicates/genotype). Overall, we conclude that *Blimp1* expression is dependent on *Neurog2*, from at least E12.5 until P2, and that our analyses are consistent with *Blimp1* mRNA and protein undergoing temporally separable regulatory mechanisms.

Neurog2 conditional mutants have a loss of rod-specific transcripts

To obtain an unbiased view of changes in gene expression in *Neurog2* retinal mutants, we generated and compared the P2 transcriptomes from control, heterozygote and mutant mice. We rationalized that our analyses at this age, shortly after endogenous expression ends, would enhance our chances of identifying *Neurog2* downstream genes. A pair of P2 retinas from each biologic replicate were used to produce libraries for high throughput sequencing (n = 5 biologic replicates/genotype). The resulting transcriptomes were analyzed using the Galaxy bioinformatics platform (www.usegalaxy.org). Those genes whose transcript levels changed significantly (Fig 8A) were further classified by ontology, using the PANTHER program (geneontology.org). The biological process categories with statistically significant changes in fold enrichment were then graphed relative to one another (Fig 8B). This analysis highlighted a set of genes, with known functions during photoreceptor development, transcriptional regulation or visual perception, which were significantly downregulated in *Neurog2* mutants (Fig. 8B). Genes labeled with an asterisk satisfied an adjusted p-value (q < 0.05), whereas the other genes showed significant downregulation (p < 0.05), but also required further validation (Fig. 8A). We selected 20 genes with differentially expressed transcripts (16 down-regulated and 4 up-regulated in hets or mutants) from the RNA-seq datasets. Those genes, indicated by gray shading in Fig 8A, were validated by qPCR among the three genotypes (Fig. 9, n > 3 biologic replicates/genotype). Overall, the RNA-seq and qPCR data were highly correlative, with the caveat that *Sag*, *Gnat1*, *Rpl11* and *Rom1* were significantly decreased in *Neurog2* mutant transcriptomic dataset (<0.5 fold change; p < 0.05), but not be validated by qPCR (Figs. 8,9). By contrast, *Id1* and *Ar11* transcript levels were upregulated in *Neurog2* retinal mutants (<0.5 fold change; p < 0.05), but also unconfirmed using qPCR (Figs. 8,9).

Interestingly, seven bHLH transcription factors were significantly downregulated in P2 *Neurog2* conditional mutants: *Atoh7*, *Neurod1*, *Neurod2*, *Neurod6*, *Olig1*, *Olig2* and *Hes2*. As proof of principle, *Atoh7* is a verified direct target of *Neurog2* (Skowronska-Krawczyk et al., 2009). But, no such information is available for the other six factors. The *Neurod* gene family generally promotes neuronal differentiation. The loss of *Neurod1* compromises rod

development while promoting bipolar genesis (Morrow et al., 1999), although this bHLH factor also acts during cone and amacrine genesis (Inoue et al., 2002; Morrow et al., 1999; Pennesi et al., 2003). *Neurod2* and *Neurod6* appear to work analogously, since overexpression of either gene at P0 promoted amacrine genesis at the expense of bipolar and Muller glial differentiation (Cherry et al., 2011). For the *Olig* genes, only *Olig2* has a clear role in a retinal neurogenesis or gliogenesis (Emerson et al., 2013; Hafler et al., 2012; Nakamura et al., 2006; Shibasaki et al., 2007). Unlike other *Hes* genes, *Hes2* retinal functions remain unknown. However, the *Hes* genes generally repress differentiation by binding to regulatory elements of proneural bHLH transcription factors (Iso et al., 2001; Sasai et al., 1992).

Of particular relevance to the *Neurog2* rod phenotype is a downregulation of eleven genes that act during rod photoreceptor differentiation or physiologic function. These genes are *Rho*, *Nr2e3*, *Gnat1*, *Sag*, *Rom1*, *Reep6*, *Psd2*, *Rs1*, *Vamp4*, *Pde6b*, *Rp111*, *Cacnalf* and *Prph2*. *Prph2* (Khan et al., 2016) and *Rom1* (Bascom et al., 1992), are critical for normal photoreceptor disk morphogenesis; while *Psd2* (Wu et al., 2016), *Reep6* (Agrawal et al., 2017) and *Vamp4* (Raingo et al., 2012) each participate in protein transport from the rod cell body to the outer segment, where light is perceived. Three other genes, *Sag* (Palczewski et al., 1989; Palczewski et al., 1992), *Gnat1* (Sauer et al., 1997), and *Pde6b* (Cote, 2004) are components of the photoactivated transduction machinery. Mutations in several of these genes are associated with human and mouse retinal dystrophies, namely *CACNA1F* (Bech-Hansen et al., 1998; Strom et al., 1998), *Gnat1* (Cameron and Lucas, 2009), *NR2E3* (Milam et al., 2002), *PDE6B* (Cheng et al., 2016), *RHO* (Dryja et al., 1990), *ROM1* (Bascom et al., 1992), *Sag/Arestin-1* (Song et al., 2013), *Rp111* (Yamashita et al., 2009), *RS1* (Huang et al., 2014; Molday et al., 2001; Molday et al., 2007; Sauer et al., 1997) and *PRPH2* (Khan et al., 2016). We also identified two factors, *Zic1* and *Ptn*, that are upregulated in P2 *Neurog2* mutant retinas. *Ptn* overexpression by electroporation of P0 rat retinas, partially blocked rod differentiation, whereas bipolar cell production was promoted (Roger et al., 2006). In retinal explants with *Zic1* overexpression, Watabe et al. (2011) found a loss of Nr2e3+ rods and an increase in cell proliferation.

Finally, because *Blimp1* mRNA and protein were significantly downregulated between E12.5 and P2 (Fig. 7), we queried the P2 *Neurog2* mutant dataset, specifically about *Blimp1* transcript levels. Consistent with our qPCR data, it was not significantly changed, further highlighted by mapping the sequence reads for all three genotypes to the *Blimp1/Prdm1* locus (Supplemental Fig. 5). It is relevant also that there was no significant change in *Nrl* mRNA levels among *Neurog2* control, het or mutant genotypes, suggesting that *Neurog2* normally regulates some aspect of rod terminal differentiation and/or neuronal function.

Discussion

In this study we used multiple *Neurog2* mutant alleles to identify a small, but significant, loss of early rod photoreceptors, and more complex, phenotypes during bipolar neurogenesis. An increase in overall number of bipolar neurons was apparent starting at P3 and persisted into adulthood. Interestingly, although rod bipolars were overproduced, there was an essentially simultaneous loss of particular cone bipolar subtypes.

Previously rodent rod photoreceptor development was shown to occur in two phases, early and late, which are separated by birth (Morrow et al., 1998). Rod precursors born during the early phase wait nearly twice as long after birth, as late phase rods, to initiate Rhodopsin expression. Interestingly, the onset of Rhodopsin expression by both cohorts of rod precursors is essentially synchronous, presumably in response to an extrinsic signal. Co-culture of these temporally distinct populations highlighted that the kinetics of early rod development are regulated cell intrinsically. Given that E17.5 *Neurog2* mutants had fewer Nr2e3+ rods, we hypothesize that this factor specifically impacts early rod formation. This is consistent with the E17.5 *Neurog2*-Cre retinal lineage producing mostly rods (Brzezinski et al., 2011), and a shutoff of *Neurog2* expression shortly after birth (Suppl Fig 1). Our data are also suggestive that *Neurog2* may be partly redundant with another factor, with *Ascl1* the most attractive candidate, given the overlap in E17.5 *Neurog2* and *Ascl1* retinal cell lineages (Brzezinski et al., 2011). However, E17.5 retinal cultures from *Neurog2*^{-/-};*Neurod1*^{-/-};*Math3/Neurod4*^{-/-} triple mutants displayed unique phenotypes whereby excess rods initially formed, but subsequently died, accompanied by a complete lack of bipolar neurons or a discernible INL (Akagi et al 2004). Thus, it would be interesting to analyze other compound bHLH factor conditional mutants to fully uncover which combinations regulate early versus late rod development.

Although both Cre drivers used in our study induced a cell autonomous loss of *Neurog2* protein at E14.5 (Suppl Fig 2), there appears to also be a simultaneous, non-autonomous loss of *Neurog2*-expressing cells. Yet, the cell autonomy of each mutant phenotype could not be easily scored, owing to the limitations of our birthdating methods. This presents a major hurdle for distinguishing between the possibilities that a) mutant retinal precursors, which normally develop as rods or cone bipolars, autonomously adopt the rod bipolar fate, or b) early postnatal mutant precursors fail to differentiate as rods, but also nonautonomously instruct nearby cells to adopt erroneous bipolar fates, before autonomously dying by P9. Moreover, loss of this somewhat minor population could nonetheless nonautonomously affect the suppression of neighboring retinal cells, sparing them from culling. We favor the second possibility that all three retinal neuron defects occur more or less simultaneously, via potentially separable molecular events but also manifest themselves at different ages. Future experiments, which mark the *Neurog2* lineage in the adult retina, will be needed to score cell autonomy of each phenotype described here.

Alternatively, *Neurog2* is known to control cell cycle exit in the brain, via its stimulation of the cyclin-dependent kinase inhibitor *p27/Kip1* (*Cdkn1b*) (Farah et al., 2000; Lacomme et al., 2012; Nguyen et al., 2006). In E12.5 *Neurog2* germline mutants, we found a longer than normal cell cycle (Maurer et al., 2018), thereby pushing the window for retinal ganglion cell differentiation. Thus, a delay in any retinal neuron birthdate might bias the genesis of relatively later cell types. If this comes into play in the postnatal retina, we propose a partially stochastic effect, where cell cycle exit delay could push committed precursor cells to erroneously differentiate as a rod bipolar. Even a short delay in terminal cell cycle exit could explain bipolar subtype phenotypes in *Neurog2* mutants, since cone bipolars normally precede rod bipolars (Morrow et al., 2008). Yet another possible explanation hinges on the relationship between the *Vsx1* and *Vsx2* gene paralogues. We discovered that while pan-bipolar markers show an overall increase in bipolar neurons, it masked the reduction of

Vsx1+ cone bipolar subtypes 1, 2, and 7 (Chow et al., 2001; Chow et al., 2004; Hayashi et al., 2000; Ohtoshi et al., 2004; Shi et al., 2011). *Vsx1* and *Vsx2* were already known to co-repress one another, for example if *Vsx2* is highly expressed by RPCs, *Vsx1* is low to non-existent (Clark et al., 2008). Therefore, in *Neurog2* retinal mutants, it would be expected that abnormally high percentages of Vsx2+ INL cells should result in fewer Vsx1+ cone bipolars. However, *Vsx1* also normally cross-represses rod bipolar cell-specific markers, including *Cabp5* and *Vsx2* (Shi et al., 2011).

The rod and bipolar phenotypes of *Neurog2* conditional mutants are similar to those of *Blimp1* (Brzezinski et al., 2010; Katoh et al., 2010), yet are clearly much less severe. Otx2+ cells that normally develop as cones or rods lack *Vsx2/Chx10* expression, thereby locking out the bipolar fate. Although it is clear that Otx2 directly activates *Blimp1* (Gloury et al., 2016; Mills et al., 2017; Wang et al., 2014), which in turn directly represses *Vsx2* (Katoh et al., 2010), this is insufficient to explain how both cones and rods arise from the *Blimp1* lineage. Here we found that as early as E12.5 a subset of *Blimp1*+ RPCs coexpresses *Neurog2*. It is potentially this group of cells that erroneously develop as bipolars in *Neurog2* mutants. One conundrum from our data is the significant reduction in *Blimp1* protein, but not mRNA, in P2 mutant retinas (Fig 7). Alternative splicing of *Blimp1* might explain this outcome (Livi and Davidson, 2006; Morgan et al., 2012; Tunyaplin et al., 2000), although we specifically amplified exon 6 which is common to all mouse *Blimp1* transcripts in the UCSC browser. Additional experiments using multiple sets of *Blimp1* qPCR primers and conditions, were unable to identify exons that might be specifically transcribed in the P2 retina. This suggests that *Neurog2* regulation of *Blimp1* transcription is stage-specific and that during early retinal development (at the peak of *Neurog2* activity) *Blimp1* transcription has some requirement for *Neurog2*. However, during postnatal retinal differentiation, particularly after *Neurog2* expression is extinguished, posttranslational regulation of *Blimp1* is more important. Given that only a subset of *Blimp1*-expressing cells depend on *Neurog2*, the underlying basis for controlling mRNA versus protein requires more investigation, including the exploration of *Blimp1* protein translation and/or turnover. However, another facet of this idea rests with *Vsx2* repression of *Blimp1* in RPCs (Reviewed in Brzezinski and Reh, 2015), which could explain the loss of *Blimp1* seen here. While there are most likely additional intrinsic factors involved, we could expect the subset of Vsx2+ *Neurog2* mutant cells that erroneously adopt a bipolar fate to downregulate *Blimp1*, thereby also contributing to the milder *Neurog2* phenotype.

Our transcriptomics analysis highlighted two genes, *Pleiotropin* (*Ptn*) and *Zic1*, whose individual gain of function phenotypes resemble that of *Neurog2* loss of function (Roger et al., 2006; Watabe et al., 2011). *Ptn* encodes a secreted heparin binding protein and, along with its paralog *Midkine* (*Mdk*), participates in neurite outgrowth in the brain (Maruta et al., 1993; Muramatsu et al., 1993; Rauvala, 1989). Studies of *Ptn* and *Mdk* suggest they are neuronal survival factors, which activate the MAPK pathway and so indirectly regulate apoptotic activity (Hida et al., 2003; Kikuchi et al., 1993; Owada et al., 1999; Satoh et al., 1993). When *Mdk* and *Ptn* are overexpressed they show neuroprotective effects in various mouse models for Parkinson's disease and Alzheimer's disease (Muramatsu, 2011). Given that *Neurog2* is crucial for dopaminergic neuron production (Kele et al., 2006), *Ptn* is an attractive candidate to act directly downstream of *Neurog2*. In the retina, *Ptn* is expressed by

both RPCs and late precursors that give rise to bipolar cells and Muller glia (Roger et al., 2006). We hypothesize that upregulation of *Ptn* in a subset of bipolar cells is neuroprotective and therefore contributes to their survival. However, Chx10-Cre;*Neurog2*^{CKO/+} retinas showed similar *ptn* upregulation as the mutants, without excess bipolar neurons, suggesting there are other critical factors that impact this phenotype.

Defects in *Zic* genes can cause a variety of congenital malformations (Aruga, 2004; Grinberg and Millen, 2005; Merzdorf, 2007). In mice, *Zic* genes 1–3 are all expressed by embryonic RPCs, and can act redundantly (Watabe et al., 2011). However, *Zic2* activity is sufficient for the correct projection of ipsilateral neurons at the optic chiasm (Aruga et al., 2002; Brown et al., 2001a). Overexpression of *Zic1*, *Zic2* or *Zic3* individually at E17 resulted in fewer rod photoreceptors, but appears to do so by blocking terminal differentiation, since excess RPCs migrated into the ONL (Watabe et al., 2011). Ectopic *Zic2* suppressed *Nr2e3* and *Nrl*, and upregulates *Id3* (Watabe et al., 2011). In *Neurog2* mutants, *Zic1* transcription was upregulated, however we could not validate changes in *M1* or *M2* levels, thus their relationship in the retina remains unresolved (Fig. 8,9). Future experiments that compare the *Neurog2* retinal cell lineage, between controls and *Neurog2* mutants are needed, to score cell autonomy of rod photoreceptor, cone and rod bipolar defects, as well as the shifts in the proportions of culled postnatal neurons. Such analyses are critical for pinpointing when and where Blimp1, the bHLH factors, rod-specific genes, *Ptn* and/or *Zic1* each require *Neurog2*.

Supplementary Material

Refer to Web version on PubMed Central for supplementary material.

Acknowledgements

The authors thank Francois Guillemot for *Neurog2*^{GFP/+} and *Neurog2*^{CKO} mice; Tom Glaser for BAC Tg Crx-Cre mice; Cheryl Craft for anti-Crx antibody; Ed Levine for anti-Vsx1 antibody; the CCHMC NextGen Sequencing and Genotyping Core; Brad Shibata, Marie-Audrey Kautzmann and April Bird for technical support; Matt Settles at the UC Davis Bioinformatics Core for help with bioinformatics data presentation; Emir Hodzic at the UC Davis Veterinary Medicine Real-Time PCR Core for help with qPCR statistical analyses; Joe Brzezinski for advice and discussions; and Anna La Torre and Joe Brzezinski for critical comments on this manuscript. This study was supported by the UC Davis Center for Vision Science NIH NEI T32 EY015387 training grant to AK, the P30 Vision Core Grant EY012576 and NIH R01 EY13612 grant to NLB.

Funding

This work supported by NEI training grant T32 EY015387 to AK; Prevent Blindness Ohio Student Fellowship to KM; P30 NEI grant EY012576; NIH R01 grant EY13612 to NLB

References

- Agrawal SA, Burgoyne T, Eblimit A, Bellingham J, Parfitt DA, Lane A, Nichols R, Asomugha C, Hayes MJ, Munro PM, Xu M, Wang K, Futter CE, Li Y, Chen R, Cheetham ME, 2017 REEP6 Deficiency Leads to Retinal Degeneration through Disruption of ER Homeostasis and Protein Trafficking. *Hum Mol Genet*.
- Akagi T, Inoue T, Miyoshi G, Bessho Y, Takahashi M, Lee JE, Guillemot F, Kageyama R, 2004 Requirement of multiple basic helix-loop-helix genes for retinal neuronal subtype specification. *J Biol Chem* 279, 28492–28498. [PubMed: 15105417]
- Aruga J, 2004 The role of *Zic* genes in neural development. *Mol Cell Neurosci* 26, 205–221 [PubMed: 15207846]

- Aruga J, Tohmonda T, Homma S, Mikoshiba K, 2002 Zic1 promotes the expansion of dorsal neural progenitors in spinal cord by inhibiting neuronal differentiation. *Dev Biol* 244, 329–341. [PubMed: 11944941]
- Bascom RA, Garcia-Heras J, Hsieh CL, Gerhard DS, Jones C, Francke U, Willard HF, Ledbetter DH, McInnes RR, 1992 Localization of the photoreceptor gene ROM1 to human chromosome 11 and mouse chromosome 19: sublocalization to human 11q13 between PGA and PYGM. *Am J Hum Genet* 51, 1028–1035. [PubMed: 1415249]
- Bech-Hansen NT, Naylor MJ, Maybaum TA, Pearce WG, Koop B, Fishman GA, Mets M, Musarella MA, Boycott KM, 1998 Loss-of-function mutations in a calcium-channel alpha1-subunit gene in Xp11.23 cause incomplete X-linked congenital stationary night blindness. *Nat Genet* 19, 264–267. [PubMed: 9662400]
- Brown LY, Odent S, David V, Blayau M, Dubourg C, Apacik C, Delgado MA, Hall BD, Reynolds JF, Sommer A, Wieczorek D, Brown SA, Muenke M, 2001a Holoprosencephaly due to mutations in ZIC2: alanine tract expansion mutations may be caused by parental somatic recombination. *Hum Mol Genet* 10, 791–796. [PubMed: 11285244]
- Brown NL, Kanekar S, Vetter ML, Tucker PK, Gemza DL, Glaser T, 1998 Math5 encodes a murine basic helix-loop-helix transcription factor expressed during early stages of retinal neurogenesis. *Development* 125, 4821–4833. [PubMed: 9806930]
- Brown NL, Patel S, Brzezinski J, Glaser T, 2001b Math5 is required for retinal ganglion cell and optic nerve formation. *Development* 128, 2497–2508. [PubMed: 11493566]
- Brzezinski JA, Reh TA, 2015 Photoreceptor cell fate specification in vertebrates. *Development* 142, 3263–3273. [PubMed: 26443631]
- Brzezinski J.A.t., Kim EJ, Johnson JE, Reh TA, 2011 Ascl1 expression defines a subpopulation of lineage-restricted progenitors in the mammalian retina. *Development* 138, 3519–3531. [PubMed: 21771810]
- Brzezinski J.A.t., Lamba DA, Reh TA, 2010 Blimp1 controls photoreceptor versus bipolar cell fate choice during retinal development. *Development* 137, 619–629. [PubMed: 20110327]
- Brzezinski J.A.t., Uoon Park K, Reh TA, 2013 Blimp1 (Prdm1) prevents re-specification of photoreceptors into retinal bipolar cells by restricting competence. *Dev Biol* 384, 194–204. [PubMed: 24125957]
- Burmeister M, Novak J, Liang MY, Basu S, Ploder L, Hawes NL, Vidgen D, Hoover F, Goldman D, Kalnins VI, Roderick TH, Taylor BA, Hankin MH, McInnes RR, 1996 Ocular retardation mouse caused by Chx10 homeobox null allele: impaired retinal progenitor proliferation and bipolar cell differentiation. *Nat Genet* 12, 376–384. [PubMed: 8630490]
- Cameron MA, Lucas RJ, 2009 Influence of the rod photoresponse on light adaptation and circadian rhythmicity in the cone ERG. *Mol Vis* 15, 2209–2216. [PubMed: 19898639]
- Carter-Dawson LD, LaVail MM, 1979 Rods and cones in the mouse retina. I. Structural analysis using light and electron microscopy. *J Comp Neurol* 188, 245–262. [PubMed: 500858]
- Cepko C, 2014 Intrinsically different retinal progenitor cells produce specific types of progeny. *Nat Rev Neurosci* 15, 615–627. [PubMed: 25096185]
- Cepko CL, Austin CP, Yang X, Alexiades M, Ezzeddine D, 1996 Cell fate determination in the vertebrate retina. *Proc Natl Acad Sci U S A* 93, 589–595. [PubMed: 8570600]
- Cheng LL, Han RY, Yang FY, Yu XP, Xu JL, Min QJ, Tian J, Ge XL, Zheng SS, Lin YW, Zheng YH, Qu J, Gu F, 2016 Novel mutations in PDE6B causing human retinitis pigmentosa. *Int J Ophthalmol* 9, 1094–1099. [PubMed: 27588261]
- Cherry TJ, Wang S, Bormuth I, Schwab M, Olson J, Cepko CL, 2011 NeuroD factors regulate cell fate and neurite stratification in the developing retina. *J Neurosci* 31, 7365–7379. [PubMed: 21593321]
- Chow RL, Snow B, Novak J, Looser J, Freund C, Vidgen D, Ploder L, McInnes RR, 2001 Vsx1, a rapidly evolving paired-like homeobox gene expressed in cone bipolar cells. *Mech Dev* 109, 315–322. [PubMed: 11731243]
- Chow RL, Volgyi B, Szilard RK, Ng D, McKerlie C, Bloomfield SA, Birch DG, McInnes RR, 2004 Control of late off-center cone bipolar cell differentiation and visual signaling by the homeobox gene Vsx1. *Proc Natl Acad Sci U S A* 101, 1754–1759. [PubMed: 14745032]

- Clark AM, Yun S, Veien ES, Wu YY, Chow RL, Dorsky RI, Levine EM, 2008 Negative regulation of *Vsx1* by its paralog *Chx10/Vsx2* is conserved in the vertebrate retina. *Brain Res* 1192, 99–113. [PubMed: 17919464]
- Cote RH, 2004 Characteristics of photoreceptor PDE (PDE6): similarities and differences to PDE5. *Int J Impot Res* 16 Suppl 1, S28–33.
- de Melo J, Clark BS, Venkataraman A, Shiao F, Zibetti C, Blackshaw S, 2018 *Ldb1*- and *Rnf12*-dependent regulation of *Lhx2* controls the relative balance between neurogenesis and gliogenesis in the retina. *Development* 145.
- Dryja TP, McGee TL, Hahn LB, Cowley GS, Olsson JE, Reichel E, Sandberg MA, Berson EL, 1990 Mutations within the rhodopsin gene in patients with autosomal dominant retinitis pigmentosa. *N Engl J Med* 323, 1302–1307. [PubMed: 2215617]
- Edgar R, Domrachev M, Lash AE, 2002 Gene Expression Omnibus: NCBI gene expression and hybridization array data repository. *Nucleic Acids Res* 30, 207–210. [PubMed: 11752295]
- Emerson MM, Surzenko N, Goetz JJ, Trimarchi J, Cepko CL, 2013 *Otx2* and *Onecut1* promote the fates of cone photoreceptors and horizontal cells and repress rod photoreceptors. *Dev Cell* 26, 59–72. [PubMed: 23867227]
- Farah MH, Olson JM, Sucic HB, Hume RI, Tapscott SJ, Turner DL, 2000 Generation of neurons by transient expression of neural bHLH proteins in mammalian cells. *Development* 127, 693–702. [PubMed: 10648228]
- Fode C, Gradwohl G, Morin X, Dierich A, LeMeur M, Goridis C, Guillemot F, 1998 The bHLH protein *NEUROGENIN 2* is a determination factor for epibranchial placode-derived sensory neurons. *Neuron* 20, 483–494. [PubMed: 9539123]
- Fossat N, Le Greneur C, Beby F, Vincent S, Godement P, Chatelain G, Lamonerie T, 2007 A new GFP-tagged line reveals unexpected *Otx2* protein localization in retinal photoreceptors. *BMC Dev Biol* 7, 122. [PubMed: 17980036]
- Gloury R, Zotos D, Zuidschewoude M, Masson F, Liao Y, Hasbold J, Corcoran LM, Hodgkin PD, Belz GT, Shi W, Nutt SL, Tarlinton DM, Kallies A, 2016 Dynamic changes in *Id3* and E-protein activity orchestrate germinal center and plasma cell development. *J Exp Med* 213, 1095–1111. [PubMed: 27217539]
- Gradwohl G, Fode C, Guillemot F, 1996 Restricted expression of a novel murine atonal-related bHLH protein in undifferentiated neural precursors. *Dev Biol* 180, 227–241. [PubMed: 8948587]
- Grinberg I, Millen KJ, 2005 The *ZIC* gene family in development and disease. *Clin Genet* 67, 290–296. [PubMed: 15733262]
- Hafler BP, Surzenko N, Beier KT, Punzo C, Trimarchi JM, Kong JH, Cepko CL, 2012 Transcription factor *Olig2* defines subpopulations of retinal progenitor cells biased toward specific cell fates. *Proc Natl Acad Sci U S A* 109, 7882–7887. [PubMed: 22543161]
- Hand R, Bortone D, Mattar P, Nguyen L, Heng JI, Guerrier S, Boutt E, Peters E, Barnes AP, Parras C, Schuurmans C, Guillemot F, Polleux F, 2005 Phosphorylation of *Neurogenin2* specifies the migration properties and the dendritic morphology of pyramidal neurons in the neocortex. *Neuron* 48, 45–62. [PubMed: 16202708]
- Hayashi T, Huang J, Deeb SS, 2000 *RINX(VSX1)*, a novel homeobox gene expressed in the inner nuclear layer of the adult retina. *Genomics* 67, 128–139. [PubMed: 10903837]
- Helmlinger D, Hardy S, Abou-Sleymane G, Eberlin A, Bowman AB, Gansmuller A, Picaud S, Zoghbi HY, Trottier Y, Tora L, Devys D, 2006 Glutamine-expanded ataxin-7 alters TFIIIC/STAGA recruitment and chromatin structure leading to photoreceptor dysfunction. *PLoS Biol* 4, e67. [PubMed: 16494529]
- Hida H, Jung CG, Wu CZ, Kim HJ, Kodama Y, Masuda T, Nishino H, 2003 Pleiotrophin exhibits a trophic effect on survival of dopaminergic neurons in vitro. *Eur J Neurosci* 17, 2127–2134. [PubMed: 12786979]
- Hinds JW, 1968 Autoradiographic study of histogenesis in the mouse olfactory bulb. I. Time of origin of neurons and neuroglia. *J Comp Neurol* 134, 287–304. [PubMed: 5721256]
- Huang Y, Mei L, Gui B, Su W, Liang D, Wu L, Pan Q, 2014 A novel deletion mutation in *RS1* gene caused X-linked juvenile retinoschisis in a Chinese family. *Eye (Lond)* 28, 1364–1369. [PubMed: 25168411]

- Hufnagel RB, Le TT, Riesenberg AL, Brown NL, 2010 Neurog2 controls the leading edge of neurogenesis in the mammalian retina. *Dev Biol* 340, 490–503. [PubMed: 20144606]
- Inoue T, Hojo M, Bessho Y, Tano Y, Lee JE, Kageyama R, 2002 Math3 and NeuroD regulate amacrine cell fate specification in the retina. *Development* 129, 831–842. [PubMed: 11861467]
- Iso T, Sartorelli V, Poizat C, Iezzi S, Wu HY, Chung G, Kedes L, Hamamori Y, 2001 HERP, a novel heterodimer partner of HES/E(spl) in Notch signaling. *Mol Cell Biol* 21, 6080–6089. [PubMed: 11486045]
- Jeon CJ, Strettoi E, Masland RH, 1998 The major cell populations of the mouse retina. *J Neurosci* 18, 8936–8946. [PubMed: 9786999]
- Katoh K, Omori Y, Onishi A, Sato S, Kondo M, Furukawa T, 2010 Blimp1 suppresses Chx10 expression in differentiating retinal photoreceptor precursors to ensure proper photoreceptor development. *J Neurosci* 30, 6515–6526. [PubMed: 20463215]
- Keeley PW, Luna G, Fariss RN, Skyles KA, Madsen NR, Raven MA, Poche RA, Swindell EC, Jamrich M, Oh EC, Swaroop A, Fisher SK, Reese BE, 2013 Development and plasticity of outer retinal circuitry following genetic removal of horizontal cells. *J Neurosci* 33, 17847–17862. [PubMed: 24198374]
- Kele J, Simplicio N, Ferri AL, Mira H, Guillemot F, Arenas E, Ang SL, 2006 Neurogenin 2 is required for the development of ventral midbrain dopaminergic neurons. *Development* 133, 495–505. [PubMed: 16410412]
- Khan AO, Al Rashaed S, Neuhaus C, Bergmann C, Bolz HJ, 2016 Peripherin mutations cause a distinct form of recessive Leber congenital amaurosis and dominant phenotypes in asymptomatic parents heterozygous for the mutation. *Br J Ophthalmol* 100, 209–215. [PubMed: 26061163]
- Kikuchi S, Muramatsu H, Muramatsu T, Kim SU, 1993 Midkine, a novel neurotrophic factor, promotes survival of mesencephalic neurons in culture. *Neurosci Lett* 160, 9–12. [PubMed: 7902544]
- Kim DS, Ross SE, Trimarchi JM, Aach J, Greenberg ME, Cepko CL, 2008 Identification of molecular markers of bipolar cells in the murine retina. *J Comp Neurol* 507, 1795–1810. [PubMed: 18260140]
- Lacomme M, Liaubet L, Pituello F, Bel-Vialar S, 2012 NEUROG2 drives cell cycle exit of neuronal precursors by specifically repressing a subset of cyclins acting at the G1 and S phases of the cell cycle. *Mol Cell Biol* 32, 2596–2607. [PubMed: 22547683]
- Le TT, Wroblewski E, Patel S, Riesenberg AN, Brown NL, 2006 Math5 is required for both early retinal neuron differentiation and cell cycle progression. *Dev Biol* 295, 764–778. [PubMed: 16690048]
- Liu C, Bakeri H, Li T, Swaroop A, 2012 Regulation of retinal progenitor expansion by Frizzled receptors: implications for microphthalmia and retinal coloboma. *Hum Mol Genet* 21, 1848–1860. [PubMed: 22228100]
- Liu IS, Chen JD, Ploder L, Vidgen D, van der Kooy D, Kalnins VI, McInnes RR, 1994 Developmental expression of a novel murine homeobox gene (Chx10): evidence for roles in determination of the neuroretina and inner nuclear layer. *Neuron* 13, 377–393. [PubMed: 7914735]
- Livak KJ, Schmittgen TD, 2001 Analysis of relative gene expression data using real-time quantitative PCR and the 2⁻($\Delta\Delta C_T$) Method. *Methods* 25, 402–408. [PubMed: 11846609]
- Livi CB, Davidson EH, 2006 Expression and function of blimp1/krox, an alternatively transcribed regulatory gene of the sea urchin endomesoderm network. *Dev Biol* 293, 513–525. [PubMed: 16581059]
- Ma Q, Kintner C, Anderson DJ, 1996 Identification of neurogenin, a vertebrate neuronal determination gene. *Cell* 87, 43–52. [PubMed: 8858147]
- Ma W, Wang SZ, 2006 The final fates of neurogenin2-expressing cells include all major neuron types in the mouse retina. *Mol Cell Neurosci* 31, 463–469. [PubMed: 16364654]
- Maruta H, Bartlett PF, Nurcombe V, Nur EKMS, Chomienne C, Muramatsu T, Muramatsu H, Fabri L, Nice E, Burgess AW, 1993 Midkine (MK), a retinoic acid (RA)-inducible gene product, produced in *E. coli* acts on neuronal and HL60 leukemia cells. *Growth Factors* 8, 119–134. [PubMed: 8466754]

- Mastick GS, Andrews GL, 2001 Pax6 regulates the identity of embryonic diencephalic neurons. *Mol Cell Neurosci* 17, 190–207. [PubMed: 11161479]
- Maurer KA, Kowalchuk A, Shoja-Taheri F, Brown NL, 2018 Integral bHLH factor regulation of cell cycle exit and RGC differentiation. *Dev Dyn*.
- Merzdorf CS, 2007 Emerging roles for zic genes in early development. *Dev Dyn* 236, 922–940. [PubMed: 17330889]
- Milam AH, Rose L, Cideciyan AV, Barakat MR, Tang WX, Gupta N, Aleman TS, Wright AF, Stone EM, Sheffield VC, Jacobson SG, 2002 The nuclear receptor NR2E3 plays a role in human retinal photoreceptor differentiation and degeneration. *Proc Natl Acad Sci U S A* 99, 473–478. [PubMed: 11773633]
- Miller MW, Nowakowski RS, 1988 Use of bromodeoxyuridine-immunohistochemistry to examine the proliferation, migration and time of origin of cells in the central nervous system. *Brain Res* 457, 44–52. [PubMed: 3167568]
- Mills TS, Eliseeva T, Bersie SM, Randazzo G, Nahreini J, Park KU, Brzezinski J.A.t., 2017 Combinatorial regulation of a Blimp1 (Prdm1) enhancer in the mouse retina. *PLoS One* 12, e0176905. [PubMed: 28829770]
- Molday LL, Hicks D, Sauer CG, Weber BH, Molday RS, 2001 Expression of X-linked retinoschisis protein RS1 in photoreceptor and bipolar cells. *Invest Ophthalmol Vis Sci* 42, 816–825. [PubMed: 11222545]
- Molday LL, Wu WW, Molday RS, 2007 Retinoschisin (RS1), the protein encoded by the X-linked retinoschisis gene, is anchored to the surface of retinal photoreceptor and bipolar cells through its interactions with a Na/K ATPase-SARM1 complex. *J Biol Chem* 282, 32792–32801. [PubMed: 17804407]
- Morgan MA, Mould AW, Li L, Robertson EJ, Bikoff EK, 2012 Alternative splicing regulates Prdm1/ Blimp-1 DNA binding activities and corepressor interactions. *Mol Cell Biol* 32, 3403–3413. [PubMed: 22733990]
- Morrow EM, Belliveau MJ, Cepko CL, 1998 Two phases of rod photoreceptor differentiation during rat retinal development. *J Neurosci* 18, 3738–3748. [PubMed: 9570804]
- Morrow EM, Chen CM, Cepko CL, 2008 Temporal order of bipolar cell genesis in the neural retina. *Neural Dev* 3, 2. [PubMed: 18215319]
- Morrow EM, Furukawa T, Lee JE, Cepko CL, 1999 NeuroD regulates multiple functions in the developing neural retina in rodent. *Development* 126, 23–36. [PubMed: 9834183]
- Muramatsu H, Shirahama H, Yonezawa S, Maruta H, Muramatsu T, 1993 Midkine, a retinoic acid-inducible growth/differentiation factor: immunochemical evidence for the function and distribution. *Dev Biol* 159, 392–402. [PubMed: 8405666]
- Muramatsu T, 2011 Midkine: a promising molecule for drug development to treat diseases of the central nervous system. *Curr Pharm Des* 17, 410–423. [PubMed: 21375488]
- Muranishi Y, Terada K, Inoue T, Katoh K, Tsujii T, Sanuki R, Kurokawa D, Aizawa S, Tamaki Y, Furukawa T, 2011 An essential role for RAX homeoprotein and NOTCH-HES signaling in Otx2 expression in embryonic retinal photoreceptor cell fate determination. *J Neurosci* 31, 16792–16807. [PubMed: 22090505]
- Nakamura K, Harada C, Namekata K, Harada T, 2006 Expression of olig2 in retinal progenitor cells. *Neuroreport* 17, 345–349. [PubMed: 16514356]
- Nguyen L, Besson A, Roberts JM, Guillemot F, 2006 Coupling cell cycle exit, neuronal differentiation and migration in cortical neurogenesis. *Cell Cycle* 5, 2314–2318. [PubMed: 17102618]
- Nishida A, Furukawa A, Koike C, Tano Y, Aizawa S, Matsuo I, Furukawa T, 2003 Otx2 homeobox gene controls retinal photoreceptor cell fate and pineal gland development. *Nat Neurosci* 6, 1255–1263. [PubMed: 14625556]
- Nowakowski RS, Lewin SB, Miller MW, 1989 Bromodeoxyuridine immunohistochemical determination of the lengths of the cell cycle and the DNA-synthetic phase for an anatomically defined population. *J Neurocytol* 18, 311–318. [PubMed: 2746304]
- Ohtoshi A, Wang SW, Maeda H, Saszik SM, Frishman LJ, Klein WH, Behringer RR, 2004 Regulation of retinal cone bipolar cell differentiation and photopic vision by the CVC homeobox gene Vsx1. *Curr Biol* 14, 530–536. [PubMed: 15043821]

- Owada K, Sanjo N, Kobayashi T, Mizusawa H, Muramatsu H, Muramatsu T, Michikawa M, 1999 Midkine inhibits caspase-dependent apoptosis via the activation of mitogen-activated protein kinase and phosphatidylinositol 3-kinase in cultured neurons. *J Neurochem* 73, 2084–2092. [PubMed: 10537068]
- Palczewski K, McDowell JH, Jakes S, Ingebritsen TS, Hargrave PA, 1989 Regulation of rhodopsin dephosphorylation by arrestin. *J Biol Chem* 264, 15770–15773. [PubMed: 2550422]
- Palczewski K, Rispoli G, Detwiler PB, 1992 The influence of arrestin (48K protein) and rhodopsin kinase on visual transduction. *Neuron* 8, 117–126. [PubMed: 1309646]
- Pennesi ME, Cho JH, Yang Z, Wu SH, Zhang J, Wu SM, Tsai MJ, 2003 BETA2/NeuroD1 null mice: a new model for transcription factor-dependent photoreceptor degeneration. *J Neurosci* 23, 453–461. [PubMed: 12533605]
- Prasov L, Glaser T, 2012 Pushing the envelope of retinal ganglion cell genesis: context dependent function of Math5 (Atoh7). *Dev Biol* 368, 214–230. [PubMed: 22609278]
- Raingo J, Khvotchev M, Liu P, Darios F, Li YC, Ramirez DM, Adachi M, Lemieux P, Toth K, Davletov B, Kavalali ET, 2012 VAMP4 directs synaptic vesicles to a pool that selectively maintains asynchronous neurotransmission. *Nat Neurosci* 15, 738–745. [PubMed: 22406549]
- Rauvala H, 1989 An 18-kd heparin-binding protein of developing brain that is distinct from fibroblast growth factors. *EMBO J* 8, 2933–2941. [PubMed: 2583087]
- Robinson JT, Thorvaldsdottir H, Winckler W, Guttman M, Lander ES, Getz G, Mesirov JP, 2011 Integrative genomics viewer. *Nat Biotechnol* 29, 24–26. [PubMed: 21221095]
- Roger J, Brajeul V, Thomasseau S, Hienola A, Sahel J-A, Guillonnet X, Goureau O, 2006 Involvement of Pleiotrophin in CNTF-mediated differentiation of the late retinal progenitor cells. *Developmental Biology* 298, 527–539. [PubMed: 16914133]
- Rowan S, Cepko CL, 2004 Genetic analysis of the homeodomain transcription factor Chx10 in the retina using a novel multifunctional BAC transgenic mouse reporter. *Dev Biol* 271, 388–402. [PubMed: 15223342]
- Sasai Y, Kageyama R, Tagawa Y, Shigemoto R, Nakanishi S, 1992 Two mammalian helix-loop-helix factors structurally related to *Drosophila* hairy and Enhancer of split. *Genes Dev* 6, 2620–2634. [PubMed: 1340473]
- Satoh J, Muramatsu H, Moretto G, Muramatsu T, Chang HJ, Kim ST, Cho JM, Kim SU, 1993 Midkine that promotes survival of fetal human neurons is produced by fetal human astrocytes in culture. *Brain Res Dev Brain Res* 75, 201–205. [PubMed: 8261612]
- Sauer CG, Gehrig A, Warneke-Wittstock R, Marquardt A, Ewing CC, Gibson A, Lorenz B, Jurklics B, Weber BH, 1997 Positional cloning of the gene associated with X-linked juvenile retinoschisis. *Nat Genet* 17, 164–170. [PubMed: 9326935]
- Seibt J, Schuurmans C, Gradwhol G, Dehay C, Vanderhaeghen P, Guillemot F, Polleux F, 2003 Neurogenin2 specifies the connectivity of thalamic neurons by controlling axon responsiveness to intermediate target cues. *Neuron* 39, 439–452. [PubMed: 12895419]
- Shi Z, Trenholm S, Zhu M, Buddingh S, Star EN, Awatramani GB, Chow RL, 2011 Vsx1 regulates terminal differentiation of type 7 ON bipolar cells. *J Neurosci* 31, 13118–13127. [PubMed: 21917795]
- Shibasaki K, Takebayashi H, Ikenaka K, Feng L, Gan L, 2007 Expression of the basic helix-loop-factor Olig2 in the developing retina: Olig2 as a new marker for retinal progenitors and late-born cells. *Gene Expr Patterns* 7, 57–65. [PubMed: 16815098]
- Sidman R, 1961 Histogenesis of mouse retina studies with thymidine-H3, in: Smelser G (Ed.), *Structure of the Eye*. Academic Press, New York, pp. 487–506.
- Skowronska-Krawczyk D, Chiodini F, Ebeling M, Alliod C, Kundzewicz A, Castro D, Ballivet M, Guillemot F, Matter-Sadzinski L, Matter JM, 2009 Conserved regulatory sequences in Atoh7 mediate non-conserved regulatory responses in retina ontogenesis. *Development* 136, 3767–3777. [PubMed: 19855019]
- Sommer L, Ma Q, Anderson DJ, 1996 neurogenins, a novel family of atonal-related bHLH transcription factors, are putative mammalian neuronal determination genes that reveal progenitor cell heterogeneity in the developing CNS and PNS. *Mol Cell Neurosci* 8, 221–241. [PubMed: 9000438]

- Song X, Seo J, Baameur F, Vishnivetskiy SA, Chen Q, Kook S, Kim M, Brooks EK, Altenbach C, Hong Y, Hanson SM, Palazzo MC, Chen J, Hubbell WL, Gurevich EV, Gurevich VV, 2013 Rapid degeneration of rod photoreceptors expressing self-association-deficient arrestin-1 mutant. *Cell Signal* 25, 2613–2624. [PubMed: 24012956]
- Strom TM, Nyakatura G, Apfelstedt-Sylla E, Hellebrand H, Lorenz B, Weber BH, Wutz K, Gutwillinger N, Ruther K, Drescher B, Sauer C, Zrenner E, Meitinger T, Rosenthal A, Meindl A, 1998 An L-type calcium-channel gene mutated in incomplete X-linked congenital stationary night blindness. *Nat Genet* 19, 260–263. [PubMed: 9662399]
- Thorvaldsdottir H, Robinson JT, Mesirov JP, 2013 Integrative Genomics Viewer (IGV): high-performance genomics data visualization and exploration. *Brief Bioinform* 14, 178–192. [PubMed: 22517427]
- Tunyaplin C, Shapiro MA, Calame KL, 2000 Characterization of the B lymphocyte-induced maturation protein-1 (Blimp-1) gene, mRNA isoforms and basal promoter. *Nucleic Acids Res* 28, 4846–4855. [PubMed: 11121475]
- Wang S, Sengel C, Emerson MM, Cepko CL, 2014 A gene regulatory network controls the binary fate decision of rod and bipolar cells in the vertebrate retina. *Dev Cell* 30, 513–527. [PubMed: 25155555]
- Wang SW, Kim BS, Ding K, Wang H, Sun D, Johnson RL, Klein WH, Gan L, 2001 Requirement for *math5* in the development of retinal ganglion cells. *Genes Dev* 15, 24–29. [PubMed: 11156601]
- Watabe Y, Baba Y, Nakauchi H, Mizota A, Watanabe S, 2011 The role of Zic family zinc finger transcription factors in the proliferation and differentiation of retinal progenitor cells. *Biochemical and Biophysical Research Communications* 415, 42–47. [PubMed: 22024047]
- Wu F, Li R, Umino Y, Kaczynski TJ, Sapkota D, Li S, Xiang M, Fliesler SJ, Sherry DM, Gannon M, Solessio E, Mu X, 2013 *Onecut1* is essential for horizontal cell genesis and retinal integrity. *J Neurosci* 33, 13053–13065, 13065a. [PubMed: 23926259]
- Wu Y, Takar M, Cuentas-Condori AA, Graham TR, 2016 *Neol* and phosphatidylethanolamine contribute to vacuole membrane fusion in *Saccharomyces cerevisiae*. *Cell Logist* 6, e1228791.
- Yamashita T, Liu J, Gao J, LeNoue S, Wang C, Kaminoh J, Bowne SJ, Sullivan LS, Daiger SP, Zhang K, Fitzgerald ME, Kefalov VJ, Zuo J, 2009 Essential and synergistic roles of *RP1* and *RP1L1* in rod photoreceptor axoneme and retinitis pigmentosa. *J Neurosci* 29, 9748–9760. [PubMed: 19657028]
- Yan RT, Ma WX, Wang SZ, 2001 *neurogenin2* elicits the genesis of retinal neurons from cultures of nonneural cells. *Proc Natl Acad Sci U S A* 98, 15014–15019. [PubMed: 11752450]
- Young RW, 1984 Cell death during differentiation of the retina in the mouse. *J Comp Neurol* 229, 362–373. [PubMed: 6501608]
- Young RW, 1985 Cell differentiation in the retina of the mouse. *Anat Rec* 212, 199–205. [PubMed: 3842042]

Highlights

- *Neurog2* is required for early rod photoreceptor, cone and rod bipolar differentiation
- Embryonic *Blimp1* expression is regulated by *Neurog2*.
- *Neurog2* has a role in postnatal retinal cell culling, particularly of bipolar neurons

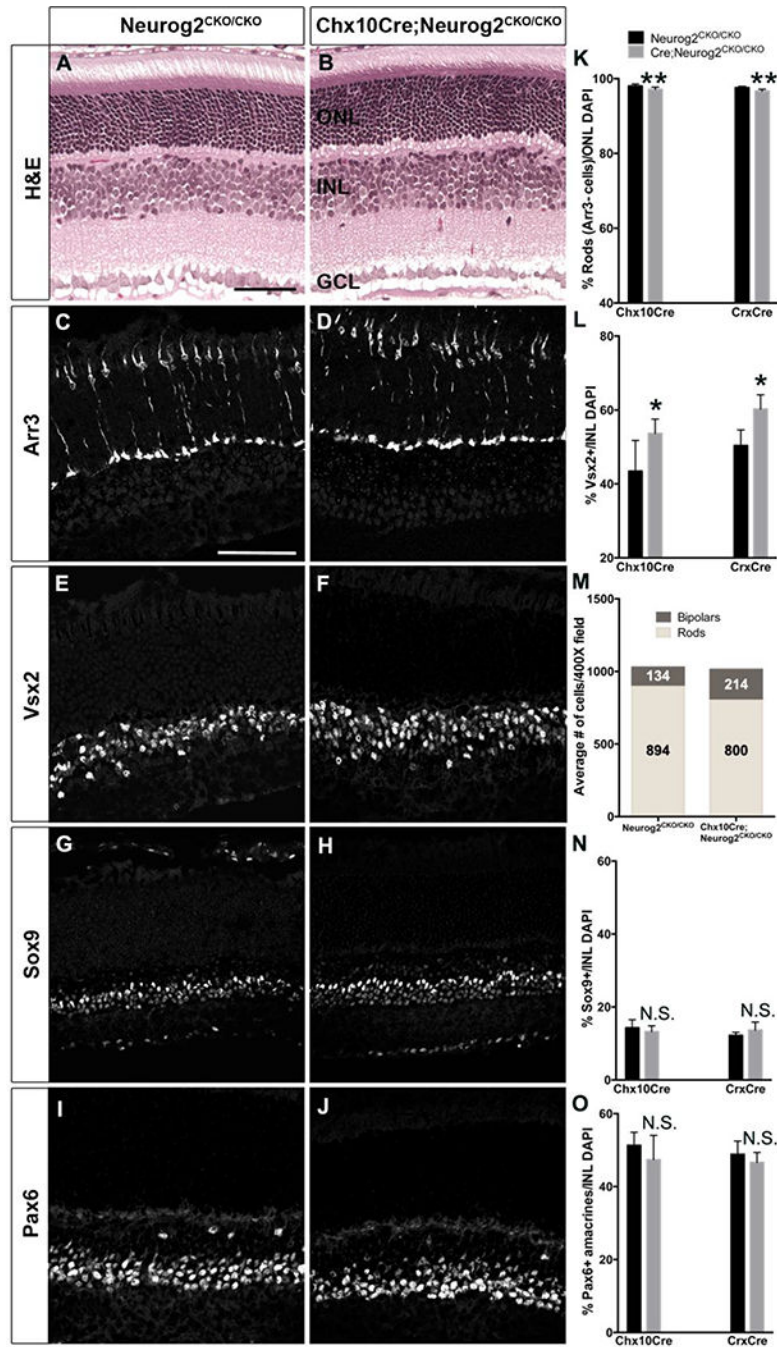


Fig. 1. Loss of rod photoreceptors in E18.5 *Neurog2* mutants.

A,B) Anti-Crx labeling of E18.5 retinal sections in both *Neurog2*^{GFP/+} and *Neurog2*^{GFP/GFP} mice. C,D) Anti-Nr2e3 labeling of nearby sections to those in A, B. E) Quantification of Crx⁺/total DAPI, Nr2e3⁺/total DAPI and Rrg⁺/total DAPI retinal cells. The Rrg data originally reported in Hufnagel et al, 2010 is regraphed here for direct comparison, (n = 3 biologic replicates/genotype; scale bar in A = 50 μ m; RPE = retinal pigmented epithelium; NBL = neuroblast layer; *P < 0.05; error bars = standard error of the mean (SEM))

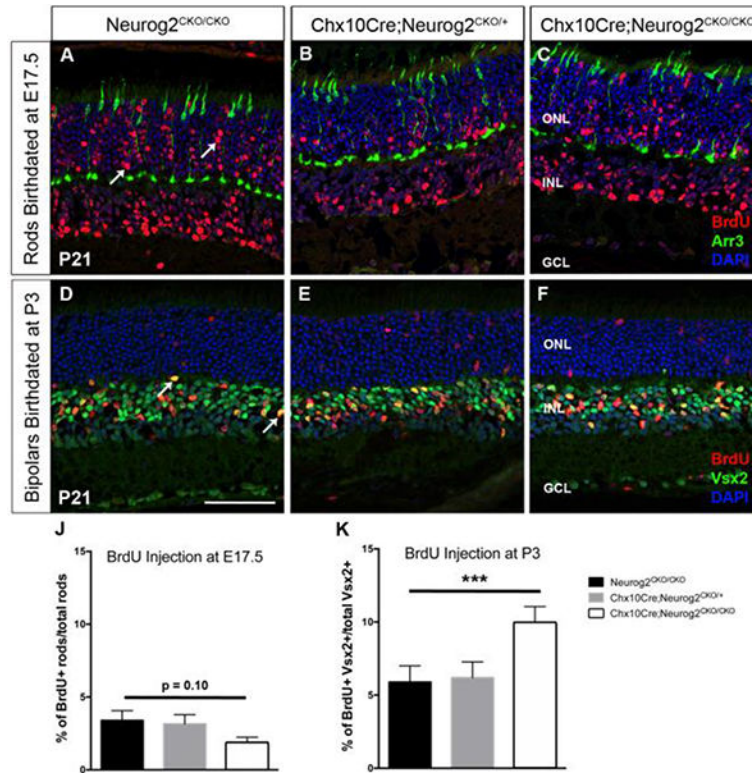


Fig. 2. *Neurog2* adult mutant retinas contain fewer rods and excess bipolar neurons. Panels A-J show P21 retinal sections.

A,B) H&E staining highlights normal retinal anatomy of Chx10- *Cre*;*Neurog2*^{CKO/CKO} eyes, compared to control littermates. C,D,K) Anti-Arr3 labeling of cone photoreceptors. Total DAPI+ ONL nuclei-total Arr3+ cones were used to estimate total number of rod photoreceptors, which was normalized over total ONL DAPI+ cells in K. E,F,L). *Vsx2*+ bipolar neurons were quantified and normalized by total INL DAPI+ cells in L. G,H,N) *Sox9*+ Muller glial cells were quantified in M. I,J,O) *Pax6*+ INL amacrine cells were normalized by total DAPI+ nuclei in N.K,L,N,O) Graphical data depict Chx10-Cre or *Crx*-Cre deletion of *Neurog2* using n= 5 biologic replicates/genotype for each Cre experiment. M) Average total counts for *Vsx2*+ bipolar and rod (*Arr3*-) cells were compared between control and Chx10-Cre;*Neurog2*^{CKO/CKO} mutants to emphasize the nearly 1:1 shift. (ONL = outer nuclear layer; INL = inner nuclear layer; GCL = ganglion cell layer; scale bars = 50 pm; **P 0.01; *P 0.05; error bars = SEM)

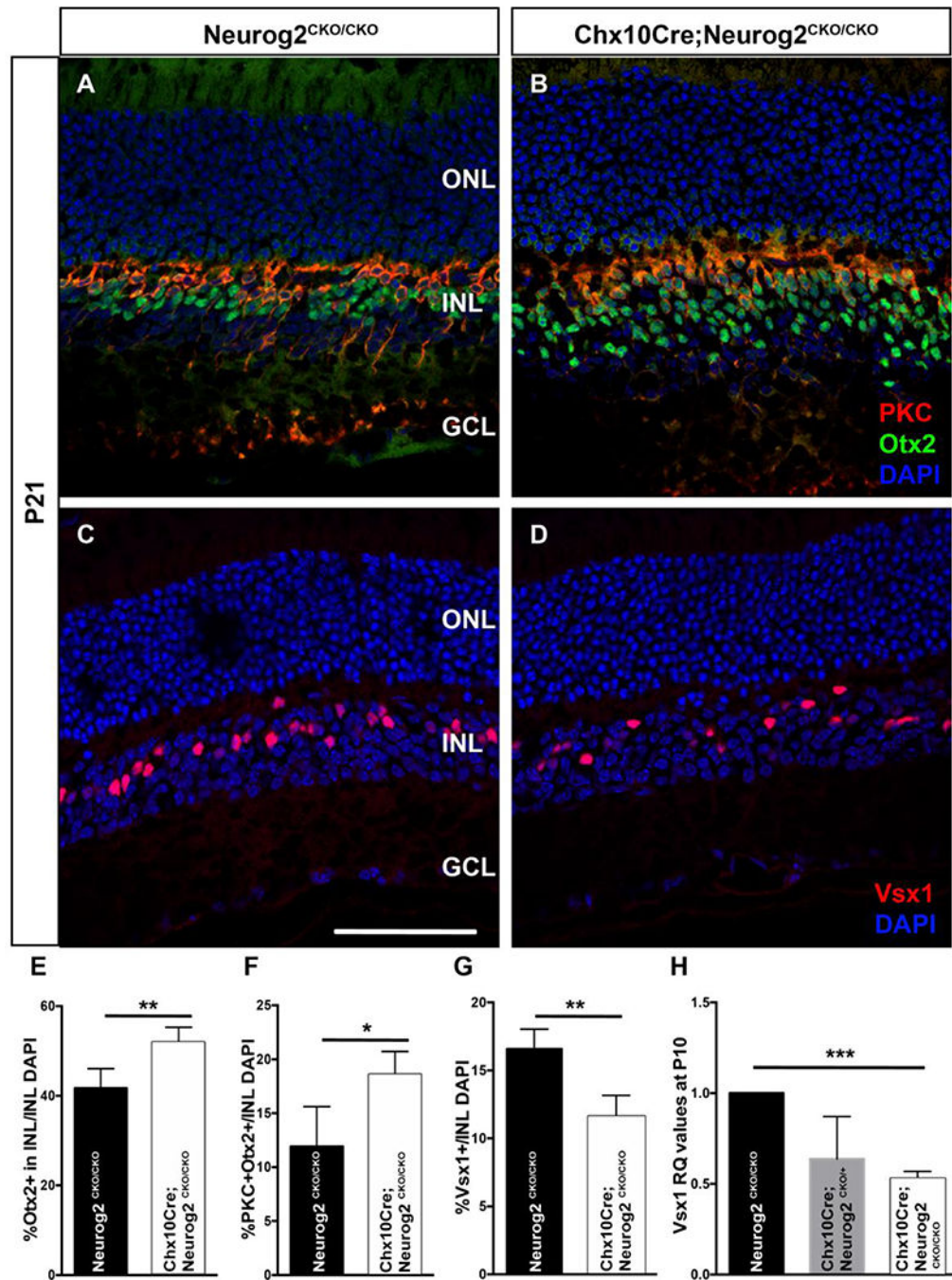


Fig. 3. E17.5 and P3 retinal birthdating of control and Chx10-Crt;Neurog2^{CKO/CKO} eyes.

A-F) Double antibody labeling for incorporated BrdU and retinal marker of interest. Quantification of rod birthdates used same strategy as P21 rods in Figure 2. A-C) Arrows point to BrdU+ rod photoreceptors (note: cones would be BrdU+Arr3+ double positive). D-F) Arrows point to examples of BrdU+Vsx2+ double positive bipolar neurons. G) Quantification of E17.5 BrdU rod data. H) Quantification of P3 BrdU bipolar data, (n = 3 biologic replicates/age and genotype; scale bar in D = 50 μ m; ***P = 0.001; error bars = SEM)

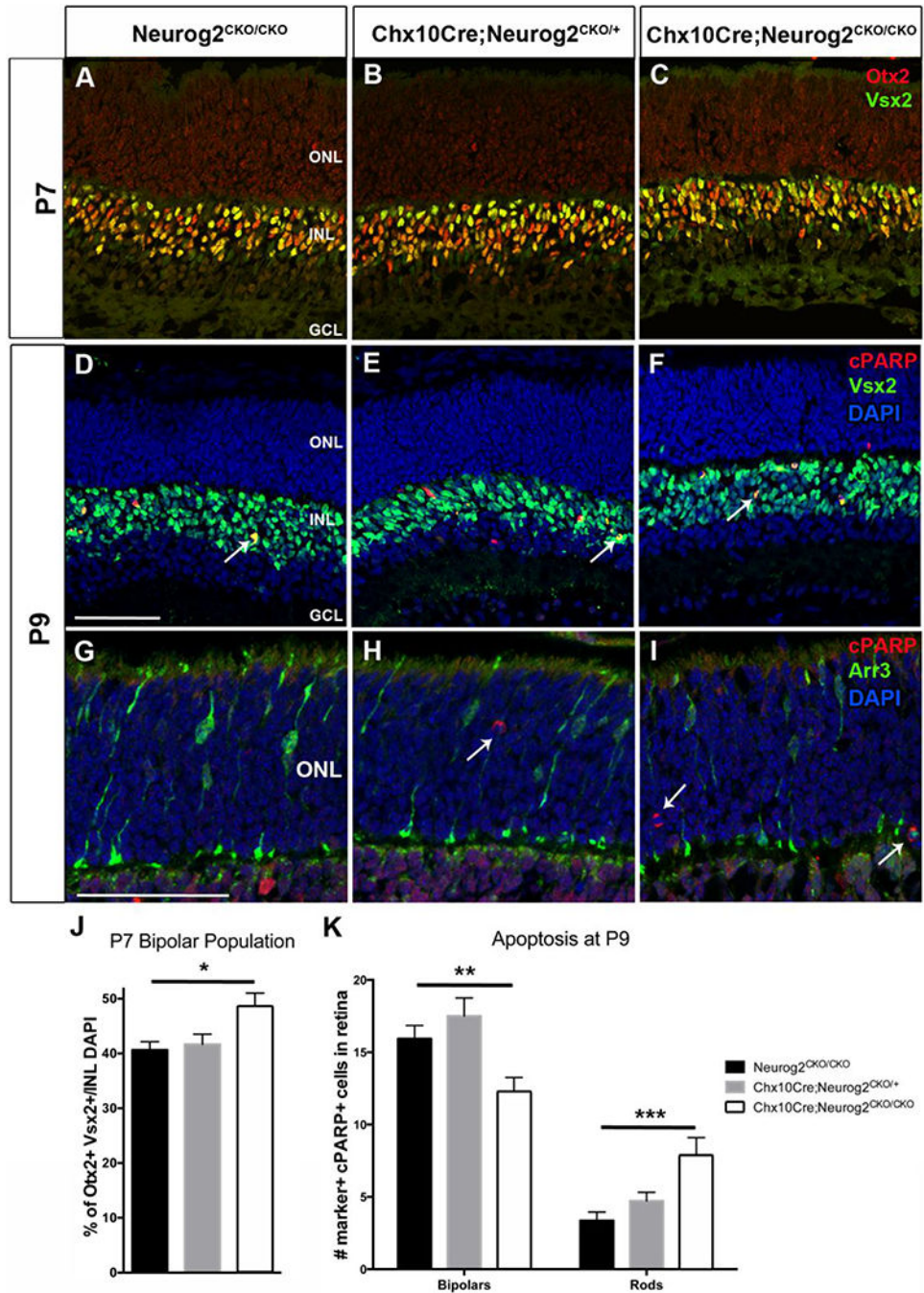


Fig. 4. Changes in proportions of bipolar subtypes in *Neurog2* mutant retinas.

Panels A-D show P21 retinal sections. A,B) Anti-Otx2 and anti-PKC colabeling of rod bipolar cells. C,D) Anti-Vsx1 labeling marks cone bipolar subtypes 1, 2 and 7 (Chow et al., 2001; Chow et al., 2004; Hayashi et al., 2000; Ohtoshi et al., 2004; Shi et al., 2011). E) The total percentage of bipolars was determined by quantifying Otx2+ INL cells versus total INL DAPI. F) The percentage of rod bipolars was determined as Otx2+PKC+ cells divided by total number of INL DAPI. G) Vsx1+ cone bipolars were divided by total INL DAPI. H) qPCR comparison of *Vsx1* mRNA in P10 wildtype and conditional het and mutant retinas,

(n = 3 biologic replicates per genotype; scale bar in C = 50 pm; ONL = outer nuclear layer; INL = inner nuclear layer; GCL = ganglion cell layer; *P 0.05; **P < 0.01; ***P 0.001; error bars = SEM)

Author Manuscript

Author Manuscript

Author Manuscript

Author Manuscript

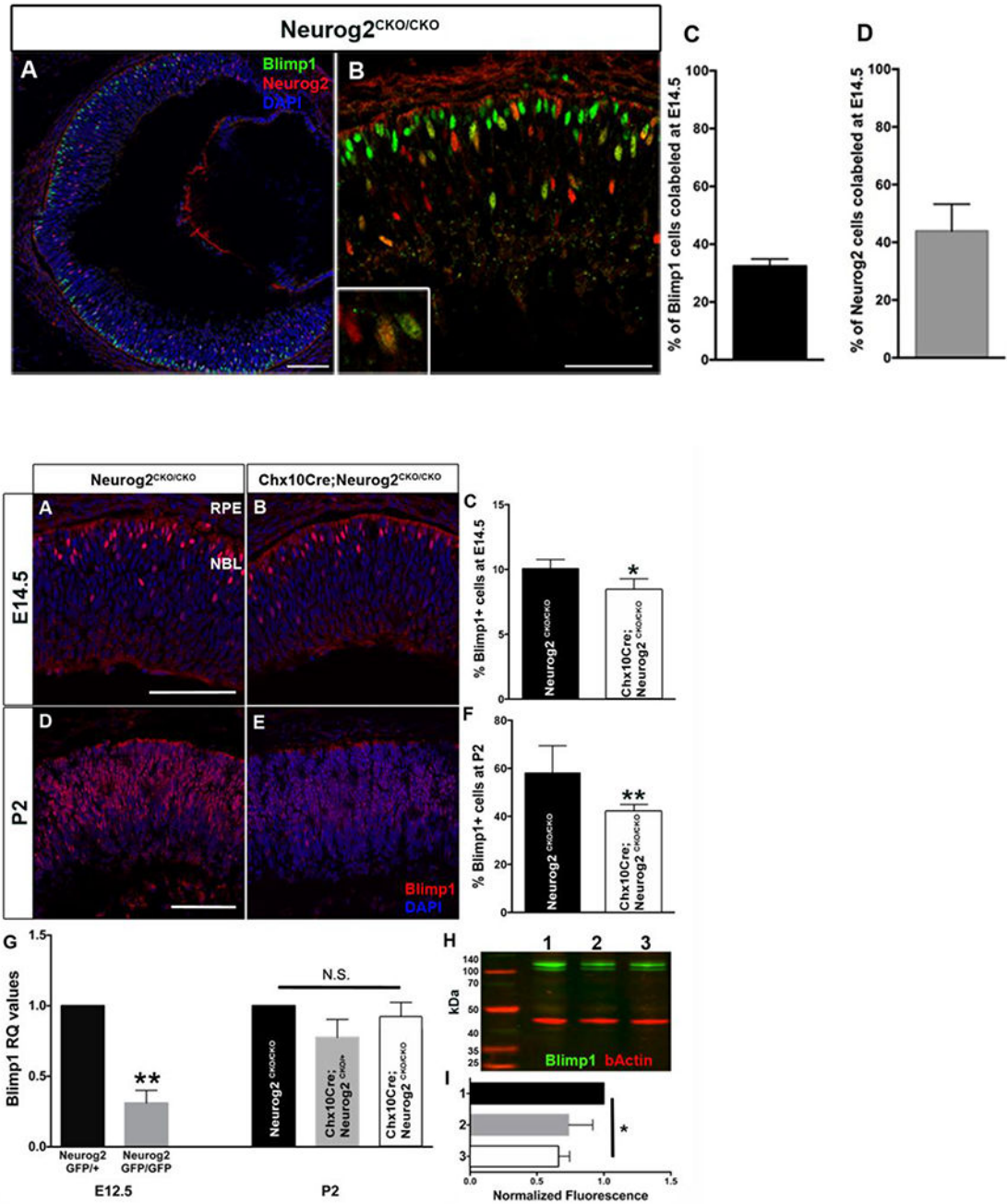


Fig. 5. P9 *Neurog2* mutant retinas have altered numbers of dying cells.

A-C, **J**) Coexpression of *Otx2* and *Vsx2* marks nascent bipolar neurons at P7 and *Otx2*+*Vsx2*+ P7 cells were normalized to total INL DAPI+ nuclei (**J**). D-F, **K**) The percentage of apoptotic INL bipolar neurons was determined using anticlaved PARP and anti-*Vsx2* colabeling (arrows). Apoptotic bipolars (cPARP+, *Vsx2*+) were normalized to total INL DAPI nuclei in entire retinal section (**K**). G-I, **K**) The percentage of apoptotic rods was quantified at P9 (cPARP+, *Arr3*- ONL cells; arrows) and normalized to total ONL DAPI nuclei per entire retinal section (**K**). (n = 3 biologic replicates per age and genotype; scale

bar in A,D = 50 μm ; ONL = outer nuclear layer; INL = inner nuclear layer; GCL = ganglion cell layer; *P 0.05; **P 0.01; ***P 0.001; error bars = SEM)

Author Manuscript

Author Manuscript

Author Manuscript

Author Manuscript

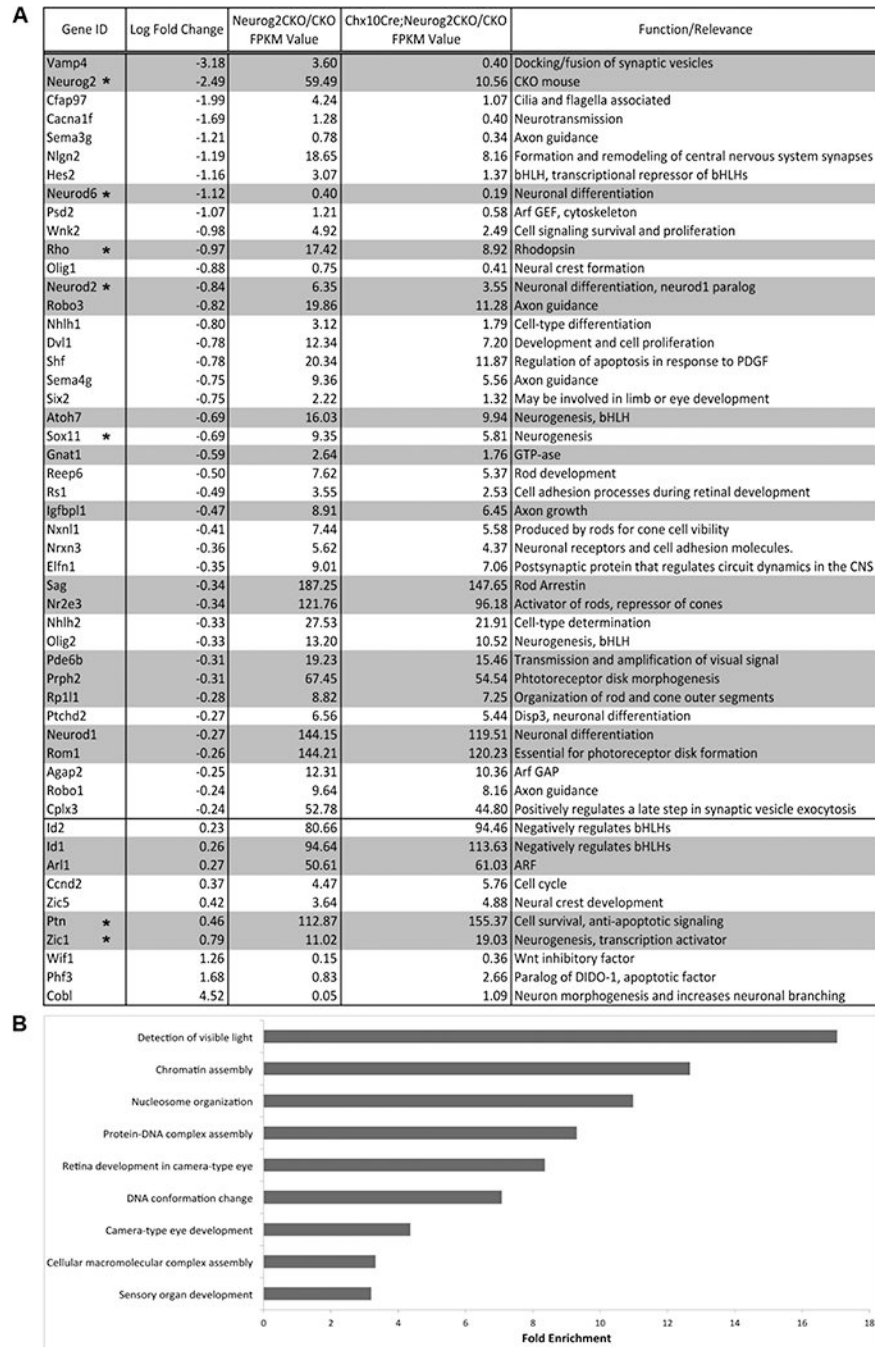


Fig. 6. Blimp1 and Neurog2 colocalization in embryonic RPCs.

A,B) Anti-Blimp1 and Anti-Neurog2 double labeling of E14.5 *Neurog2* wild type retina. A) Both Blimp1 and Neurog2 are expressed by a subset of E14.5 RPCs. B) Each single labeled population, and the colabeled fraction are also shown at higher magnification. C,D) Co-expressing cells (Blimp1+Neurog2+) were quantified within the Blimp1+ population (C) and within the Neurog2+ population (D). (n = 3 biologic replicates; scale bar in A = 100 pm; in B = 50 μ m; error bars = SEM).

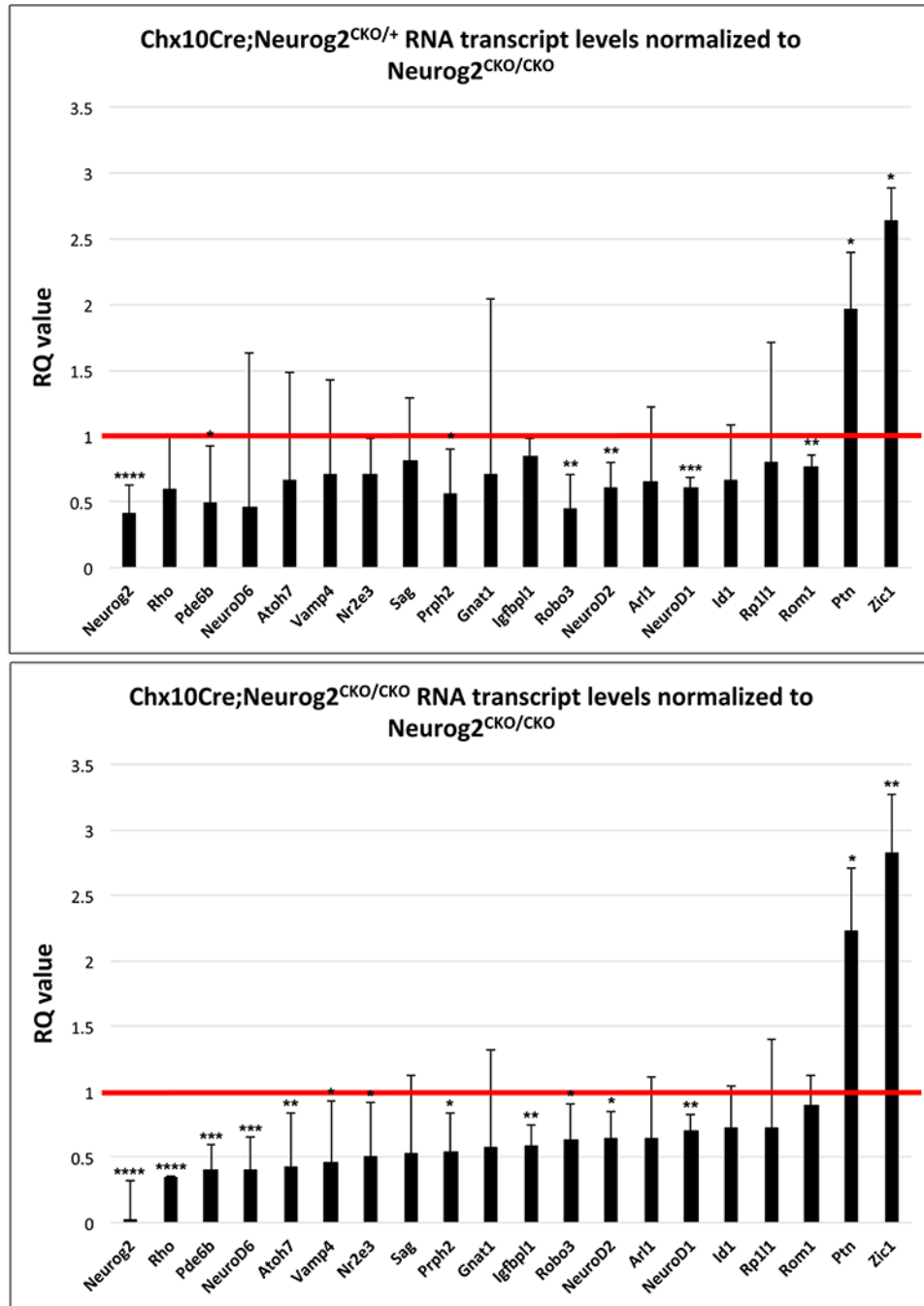


Fig. 7. *Blimp1* mRNA and protein levels are affected across multiple ages of *Neurog2* mutants. A-C) Anti-*Blimp1* labeling of E14.5 RPCs in A,B; quantified in C for controls and *Chx10-Cre;Neurog2^{CKO}* mutants. D-F) Expression and quantification of P2 *Blimp1*⁺ cells (n=3/genotype). G) qPCR comparison of *Blimp1* mRNA in GFP⁺ E12.5 *Neurog2^{GFP/+}* and *Neurog2^{GFP/GFP}* RPCs, along with qPCR comparison of *Blimp1* mRNA from P2 retinas from littermates. Although P2 data is not statistically significant, there is a trend towards lower *Blimp1* transcript levels (n= 3/age + genotype). H) Western blot of *Neurog2^{CKO/CKO}* (1) *Chx10-Cre;Neurog2^{CKO/+}* (2) and *Chx10-Cre;Neurog2^{CKO/CKO}* (3) P2 retinal total

protein, labeled with antibodies against Blimp1 and β -Actin. I) Quantification of western blot signal strength by densitometry (genotypes labeled as in H). Anti-Blimp1 was normalized versus anti- β -Actin. *Neurog2^{CKO/CKO}* controls were normalized to 1 and *Chx10-Cre;Neurog2^{CKO/+}* and *Chx10-Cre;Neurog2^{CKO/CKO}* intensities portrayed versus that value (n = 3 biologic replicates/age + genotype; RPE = retina pigment epithelium; NBL = neuroblast layer; kDa = kilodaltons; scale bars in A,D = 50 μ m; *P < 0.05; **P < 0.01; error bars = SEM)

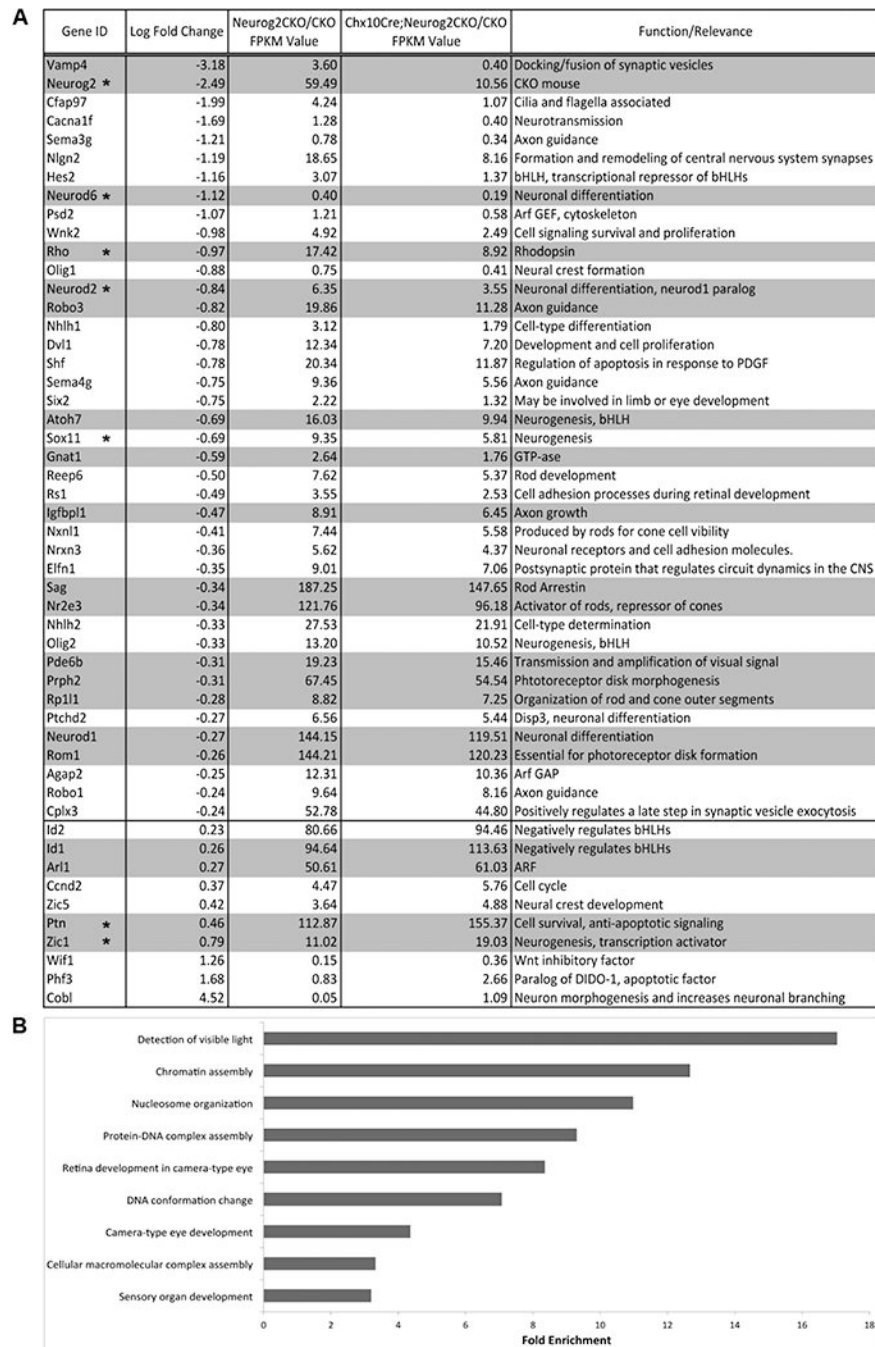


Fig. 8. Transcriptomics of P2 *Neurog2*^{CKO/CKO}, *Chx10-Cre; Neurog2*^{CKO/+} and *Chx10-Cre Neurog2*^{CKO/CKO} retinas.

A) Selected genes from P2 RNA-seq dataset analyses of *Chx10-Cre; Neurog2*^{flox} wild type, heterozygote and mutant retinas (n = 5 biologic replicates/genotype). The log-fold change between genotypes is provided. Values in control and mutant columns represent fragments per kilobase of transcript per million mapped reads (FPKM). All transcripts have a significance of p < 0.05. Transcripts with a significant adjusted p-value (*q < 0.05) are denoted with an asterisk. Those genes validated by qPCR are shown with gray highlighting. The demonstrated or predicted function of each gene is listed in the rightmost column. B)

Transcripts were analyzed with gene ontology with only those categories of significance ($p < 0.05$) displayed. Functional groups were ranked by fold enrichment.

Author Manuscript

Author Manuscript

Author Manuscript

Author Manuscript

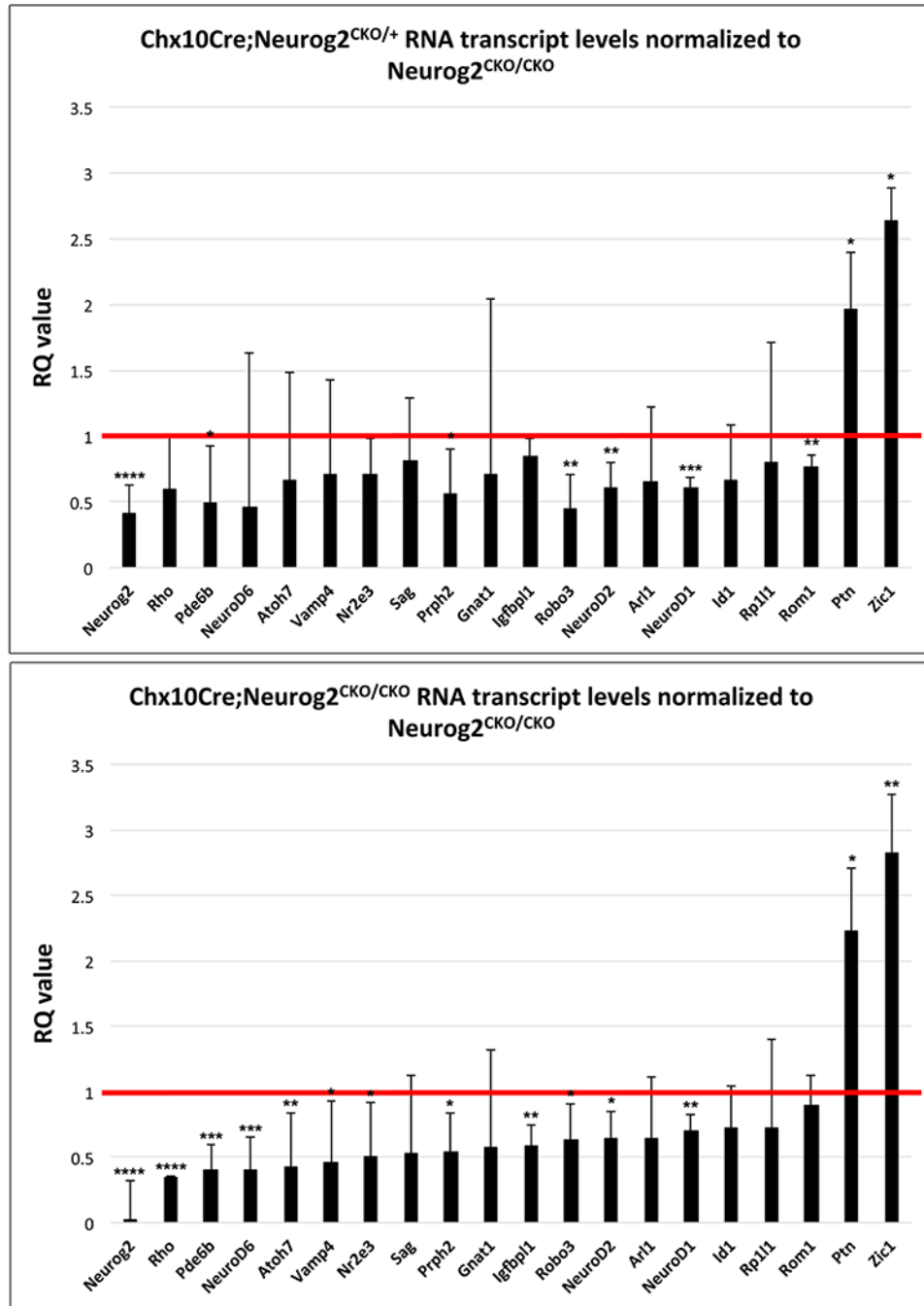


Fig. 9. qPCR validation of gene transcript levels in P2 retinas.

Differentially expressed gene transcripts of interest (see Fig 8) were quantified by qPCR among *Neurog2^{CKO/CKO}*, *Chx10-Cre;Neurog2^{CKO/+}* and *Chx10-Cre;Neurog2^{CKO/CKO}* individuals. A) Direct comparison of *Neurog2^{CKO/CKO}* control and *Chx10-Cre;Neurog2^{CKO/+}* heterozygote mRNA levels. B) Direct comparison of *Neurog2^{CKO/CKO}* control and *Chx10-Cre;Neurog2^{CKO/CKO}* mutant mRNA levels. Mean relative quantification (RQ) values were calculated by normalizing mutant and heterozygote RNA levels to their counterpart wild type RNA levels (shown as a red line at 1.0). Error bars represent standard

error of the mean, (n = 3 biologic replicates/genotype; *P < 0.05; **P < 0.01; ***P < 0.001; ****P < 0.0001; error bars = SEM)

Author Manuscript

Author Manuscript

Author Manuscript

Author Manuscript